TRACOR 6500 TRACOR LANE, AUSTIN, TEXAS 78721

Document Number 69-267-U

TECHNICAL NOTE

A NULL STEERING TECHNIQUE FOR INTERFERENCE REJECTION.

1969

TABLE OF CONTENTS

1. INTRODUCTION

Plane wave interfering sources have long posed problems to our sonar signal processors' performance. This interference is generally caused by such things as (1) secondary or multiple targets within the detection/classification range envelope of the sonar system; (2) convoys which the ship carrying the sonar is screening; (3) jammers released by a target as a countermeasure; and (4) torpedoes fired by own ship. As sonar systems are improved and detection ranges become longer, this increased sensitivity to targets also implies an increased sensitivity to interference. Since both are plane waves which propagate across the array, and since the basic purpose of beamforming is to discriminate against the spatially incoherent noise and enhance coherent plane waves, it might at first seem to be a rather hopeless situation. However, the supposition in beamforming, as in all signal processing, is simply to discriminate against signal and noise based upon the differences between their spatial and temporal characteristics. It is possible, in general, to discriminate against signal and noise (or as the case may be, to discriminate against signal-plus-noise and noise only) based upon spectral, waveform, statistical, and spatial organization differences. The interference problem may be treated in any or all of these categories. In order to dermine how best to cope with this problem, it is instructive to talk about the problems which interfering noises cause in the attainment of good (or if one prefers optimal in some sense) sonar performance.

The performance of a sonar system should be measured or predicted based upon how well the system meets its specific objectives. The two primary objectives of a sonar are to detect and classify targets as soon as possible and at the greatest range possible. Target localization, in range and bearing, and target tracking are also important even if secondary objectives. Only the two primary objectives (detection/classification) will be

discussed here; however, many of the same problems, and perhaps similar solutions, exist in the achievement of the many secondary objectives in sonar performance.

Consider first the detection of plane wave signals in the presence of noise which consists of a more or less spatially uniform background plus one or more plane wave interfering noises, which have relatively high power levels compared with the signal and/or spatially uniform noise background. If the elements in the receiving array are beamformed by classical time shift and sum methods, the spatially uniform background noise is discriminated against to some extent, roughly incoherently summed, while a signal arriving from on or very near the beam boresight bearing is alligned in phase by the time shifts and coherently summed. Naturally, if a plane wave inferfering noise source lies very near the plane wave signal bearing, there is very little chance that their spatial organizations are enough different to effectively discriminate between the two. In that case, there is hopefully some way to discriminate between the two based upon spectral, waveform, or statistical differences. However, if the plane wave interfering noise is located at a bearing different from the signal bearing, it has been somewhat decorrelated at the output sum of the time shifted elements. The side lobe levels of the beamformed array beam patterns are a measure of how much decorrelation has taken place. For typical passive receiving arrays and frequency bands, these levels are generally no more than -10 dB to -15 dB below the boresight direction response. Thus, if a plane wave interfering noise source has a higher power level than the signal by an amount much greater than the side lobe level, it can present severe problems in the detection of the signal. Depending on the particular hardware implementation of the rest of the system, the problems which it causes may differ. However, typically these are:

(1) The system may lose normalization,

(2) The system may be driven out of its useful dynamic range, and

(3) Signal masking will occur.

For the case of passive broadband detection and passive narrowband spectral line detection of the target the three above problems are considered to be serious.

Considering the classification objectives of a sonar system leads to the same basic problems caused by plane wave interfering noises. The problems associated with (3) above are probably most noticeable to a classification sonar operator. Since passive target classification is based primarily on spectral line signatures there will obviously be a fourth problem presented by interfering secondary targets in the case of target classification. The classification display will contain the superposition of more than one target signature which the operator must somehow separate prior to being able to classify the primary target signature. The following section discusses several approaches which have been applied to these problems.

2. BACKGROUND

The following paragraphs contain a discussion of several classical and some more recent approaches to the solution of problems posed by plane wave interfering sources.

2.1 Classical Approaches

One of the oldest approaches to the problem of interference is to filter the outputs of the receiving elements of the array into a frequency band where the interference is not so severe. Applications of this approach are most often found in active sonars. This reduces interference from other ships operating in close proximity which normally transmit in the same frequency band. This approach is also useful for detection of high relative doppler targets in reverberation limited situations. This scheme is also useful in passive sonars when sinusoidal or narrowband jammers are the source of interference.

When the interference is as broadband as the targets to be detected there is no advantage to the above approach. Increasing the number of quantizing levels at the element outputs and automatic gain controlling (A.G.C.) prior to quantization is often necessary in detection systems to prevent them from being driven out of their useful dynamic range and losing time normalization. Rethresholding of the system is often accomplished to prevent display saturation through the use of post beamformer spoke suppressors. All of these approaches simply give up detection range in the presence of interference in order to remain useful at least for shorter detection ranges. The simple approach of adding independent noise prior to quantizer inputs has even been suggested. This emphasizes the fact that many approaches thus far posed are willing to sacrifice the detection sensitivity in order to remain useful.

An approach which attacks the problem more fundamentally is that of array shading to suppress the side lobe levels. Array element outputs may be weighted in a prescribed fashion prior to

time shifting and summing to reduce the response of the system to plane waves arriving from angles far removed from the major response axis of the beams. The two shading techniques which have been classically applied to sonar array processors are Taylor shading and Dolph-Tchebyscheff shading. Taylor shading produces asymptotically decreasing side lobe levels moving away from the major lobe. Dolph-Tchebyscheff shading produces uniformly low prescribed side lobe levels. The second technique should be considered more desirable if the angle of arrival of the interference is unknown. The first technique could be considered more desirable if it is known that interference is more likely to occur from directions farther removed from the beam boresight. In the case of passive preformed beam receivers covering 360° of azimuth, the Dolph-Tchebyscheff technique would be more appropriate.

Suppression of side lobes causes two things to happen which can be considered undesirable. The first is that the array gain in the presence of a uniform noise background is degraded. The second undesirable feature of shading is the characteristic broadening of the major lobe. Thus, the system will have less bearing resolution and be more susceptible to interference arriving from larger angles relative to the major response axis.

When an interfering noise source is arriving from a direction far removed from the beam boresight direction the shaded array will produce a lower noise output due to interference than an unshaded array. Typical side lobe levels for shaded arrays are -25 dB. Thus, the interfering noise in the beam output will be 10 or 15 dB below the level which would be obtained if simple unshaded time shift and sum beamforming were used. Thus, the problems due to interference have been reduced. It should be remembered that shading is accomplished at the quantized element outputs if one anticipates a digital beamformer. Thus, if the array elements' outputs are quantized prior to beamforming, there is still a problem with the quantizer inputs being driven out of

their dynamic range unless A.G.C.'s are used. Since A.G.C.'s are combinations of estimators and non-zero lag time feedback mechanisms, their inherent errors often result in poor system performance due to mis-normalization. For this reason, it is often desirable to clip the element outputs. While this would not necessarily preclude shading, clipping of the element outputs when they are dominated by high level interference will result in the array processor operating in a non-linear region and poor performance will result.

2.2 Recent Approaches

There have been several approaches to the removal of interference as an integral part of array processors. While these techniques have been suggested in the literature many years hence, they have only recently been applied to sonar array processing. A few of the more pertinent techniques are described below.

Victor C. Anderson has described and developed a technique for the removal of interference based upon an estimate of the interfering waveform. Briefly, the system forms a beam in the direction of the interference through time shift and summing the outputs of array elements which have been 12 bit quantized. The estimate of the interfering waveform produced at this beam output is subtracted (after appropriate re-normalization) from the 12 bit quantized outputs of all the staves. After this subtraction, the outputs are then clipped (sign bit only is retained) time shifted to phase up to the beam boresight directions and summed. Thus, the interfering waveform is removed prior to clipping. This technique should work well at least for removal of highly structured interfering waveforms such as sinusoidal jammers. This equipment is quite complex in practice and is somewhat limited in the types of interference for which it will be applicable.

Morton Kanefsky [1] has recently suggested that the problems due to interference in a clipped system might more simply be reduced by subtracting elements pair wise after clipping and time delaying so that the interference is in phase at the two inputs to the difference junction. If the input statistics to the clippers are gaussian, summing of the two clipper outputs yields an output autocorrelation function given by:

$$R_c^+(\tau) = \frac{2}{\pi} \sum_{i=1}^{2} \sum_{j=1}^{2} \text{Sin}^{-1} \frac{R_{ij}(\tau)}{\left[R_{ii}(0)R_{jj}(0)\right]^{\frac{1}{2}}} , \qquad [2\text{-}1]$$

where the $R_{ij}(\tau)$'s are the correlation functions between elements i and j at the clipper inputs. For $i = j$ these are the autocorrelation functions and for $i \neq j$ they are the cross correlation functions between the two channels. Subtracting the two outputs of the clippers yields

$$R_c^-(\tau) = \frac{2}{\pi} \sum_{i=1}^{2} \sum_{j=1}^{2} (-1)^{i+j} \text{Sin}^{-1} \frac{R_{ij}(\tau)}{\left[R_{ii}(0)R_{jj}(0)\right]^{\frac{1}{2}}} . \qquad [2\text{-}2]$$

Examination of equations [2-1] and [2-2] shows that when the two elements that are clipped contain a significant amount of correlated noise (plane wave interference) the difference of the clipped elements produces a lower output as can be seen by writing the two equations as indicated below:

$$R_c^+(\tau) = \frac{2}{\pi} \left\{ \text{Sin}^{-1} \left[\frac{R_{11}(\tau)}{R_{11}(0)}\right] + \text{Sin}^{-1} \left[\frac{R_{22}(\tau)}{R_{22}(0)}\right] + 2 \text{Sin}^{-1} \left[\frac{R_{12}(\tau)}{\left[R_{11}(0)R_{22}(0)\right]^{\frac{1}{2}}}\right] \right\} , \qquad [2\text{-}3]$$

and

$$R_c^-(\tau) = \frac{2}{\pi}\left\{\mathrm{Sin}^{-1}\left[\frac{R_{11}(\tau)}{R_{11}(0)}\right] + \mathrm{Sin}^{-1}\left[\frac{R_{22}(\tau)}{R_{22}(0)}\right] - 2\,\mathrm{Sin}^{-1}\left[\frac{R_{12}(\tau)}{\left[R_{11}(0)R_{22}(0)\right]^{\frac{1}{2}}}\right]\right\} . \qquad [2\text{-}4]$$

The noise powers out of the sum and difference junctions are given by the zero lag (τ=0) value of R_c^+ and R_c^- respectively. Normalizing such that $R_{11}(0) = R_{22}(0) = 1$,

$$R_c^+(0) = \frac{2}{\pi}\left\{2 + 2\,\mathrm{Sin}^{-1}\left[R_{12}(0)\right]\right\} \qquad [2\text{-}5]$$

and

$$R_c^-(0) = \frac{2}{\pi}\left\{2 - 2\,\mathrm{Sin}^{-1}\left[R_{12}(0)\right]\right\} .$$

Highly correlated plane wave noise arriving at the array will cause $R_{12}(0)$ to be a positive quantity for adjacent element spacings less than $\frac{\lambda}{2}$ and for almost all interference arrival angles even for element spacings equal to $\frac{\lambda}{2}$, where λ is the wave length of the effective center frequency of the band being processed. Thus since $\mathrm{Sin}^{-1}[\theta] > 0$ for $\theta > 0$, $R_c^-(0)$ produces a lower output than $R_c^+(0)$. For $R_{12}(0) \sim 1.0$ [i.e., for element cross correlations essentially dominated by plane wave interference] $R_c^-(0)$ approaches zero. Therefore the higher the interference the better job of removing noise the processor accomplishes. However, the non-linearities introduced prior to removal of the interference can yield this system unusable since increases in the element cross-correlations due to additive signal do not produce proportionate increases in the value of the output autocorrelation function. Thus, the plane wave noise is driving the beamformer into saturation at the output so that signal can not

be detected for the high interference situation for which the null-steering processor removes noise the best. Kanefsky suggests that the element positions be considerably greater than $\frac{\lambda}{2}$ to alleviate some of the seriousness of this problem. However, this implies building larger arrays in order to process the same frequency bands in the presence of interference. The case of sinusoidal interference will still present a problem for these larger element spacings since the cross-correlation at the element outputs due to this type of interference is not in general reduced by the increased separation.

The subject of this paper is a technique very similar to that above for the removal of interference prior to clipping if a clipped beamformer is in order. If a more linear beamformer (multi-bit) is proposed, then the null-steering technique described in Section 3 would be utilized prior to the element output quantizing to alleviate dynamic range problems which, of course, are less serious in the multi-bit than the hard clipped systems. The array element spacings for either case can be less than $\frac{\lambda}{2}$ without suffering significant problems due to system non-linearities or dynamic range considerations.

Mermoz[2] has developed the linear multi-channel matched filter system which is optimum in the sense that when the outputs of N filters, one for each element, are summed, the output of the sum provides the highest output signal-to-noise ratio possible.

For the case of a noise correlation matrix for the N element outputs caused by $M \leq N-1$ interfering plane wave noise sources, Mermoz concluded[2] that the matched filter system resulted in the simultaneous elimination of the noise and the signal at the output since all filter weights become identically equal to zero. More recently, Mermoz has shown[3] that if one takes the approach of finding the set of filters which totally eliminates this class of noise without simultaneously eliminating the signal, that in general such a set of filters do indeed exist. The N filters which

result consist of no more than M delays (taps) with weights which are identical within a sign on alternate elements in the array. Thus, the filters produce M nulls in the array response (beam pattern) in the direction of the interfering noise sources.

The description of the system which follows in the next section is a system which provides some number, $M \leq N-1$, of nulls in the array response pattern which are simply adjustable either by an operator or adaptively when interfering plane wave noise sources are limiting system performance. A comparison of the performance of this interference rejection technique is provided in Section 4 using a time shift and sum beamformer as a reference. The examples provided in that section are for the more realistic case of an isotropic noise plus some number of plane wave sources at various intensities relative to the isotropic background.

3. DESCRIPTION OF TECHNIQUE FOR INTERFERENCE REJECTION

The interference rejection technique described in this section is a simple and realizable addition to present time shift and sum sonar array beamformers which can improve system gain and thus improve detection performance in the presence of high level interfering plane wave noise sources. Classification performance, at least for passive spectrum analysis techniques, may also be considerably improved by the use of this technique since it can be used to eliminate secondary target spectra from the classification display when the secondary target arrival direction differs from the primary target arrival direction.

The beamforming technique described herein consists of time delaying adjacent element pairs so that the interference is identical at the time delayed outputs and then subtracting adjacent time delayed outputs. This may be viewed as forming an effective directional receiving element at the centers of the line adjoining each of the element pairs. All of these directional elements are then time delayed such that the signal arriving from the desired boresight direction is in phase at the newly formed directional receiving element outputs, and all outputs are summed to form a beam. The new directional receiving elements have a null response in the direction of the interference and thus the interference is eliminated from the beam output. A set of preformed beams may be provided by providing sets of beam boresight delays (one set for each preformed beam) to be applied to the newly formed directional elements prior to summing.

The technique may be extended to provide directional elements for time shifting and summing which have more than one null in their response pattern and thus multiple interfering plane wave sources may be eliminated from the beam outputs.

3.1 Formation of Directional Receiving Elements with One Null

Consider a line array of N equally spaced (d) omni-directional point receiving elements. In order to provide directional receiving elements which have a null response in the direction θ, a system such as that shown in Figure 3-1 may be utilized.

As the Figure 3-1 illustrates, the N element array of omni-directional receiving elements may be processed in such a manner as to form N-1 outputs which may be time shifted and summed to form a beam in the desired boresight direction. Let the waveform at the output of the k^{th} element in this array in the presence of monochromatic noise arriving from a direction φ be

$$S_k(t) = \text{Cos}\,[\omega t + X_k(\varphi)]\,, \qquad [3\text{-}1]$$

where $$X_k(\varphi) = \frac{2\pi d_k}{\lambda}\,\text{Cos}\varphi$$

and d_k is the distance from some arbitrary orgin about which the angle φ is measured. Picking this arbitrary orgin to be the first element in the line array the element outputs are given by

$$S_k(t) = \text{Cos}\,[\omega t + (k-1)X(\varphi)] \qquad [3\text{-}2]$$

since $d_k = d(k-1)$ and where $X(\varphi) = \frac{2\pi d}{\lambda}\,\text{Cos}\varphi$

The time delays, τ_1 in Figure 3-1 are picked such that a plane wave arriving from an angle $\varphi = \theta_1$ is in phase with the undelayed adjacent element output. Thus, where c is the propagation velocity of the medium,

$$\tau_1 = \frac{d}{c}\,\text{Cos}\theta_1, \qquad [3\text{-}3]$$

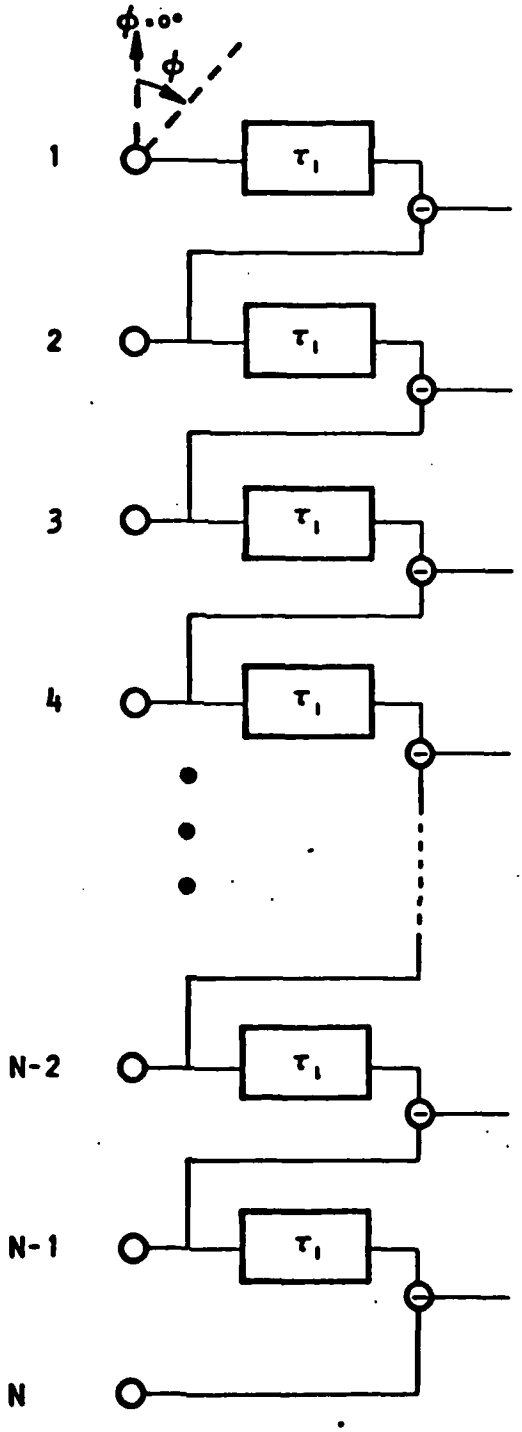

FIG. 3-1 SCHEMATIC REPRESENTATION OF A ONE NULL PROCESSOR.

and the waveform at the k^{th} delayed element output is given by

$$S_k'(t) = \text{Cos}[\omega t + (k-1)X(\varphi) + X(\theta_1)], \qquad [3\text{-}4]$$

where $X(\theta_1) = \frac{2\pi d}{\lambda} \text{Cos}\theta_1$.

The difference of the adjacent element outputs is then given by

$$S_k'(t) - S_{k+1}(t) = \text{Cos}[\omega t + (k-1)X(\varphi) + X(\theta_1)] - \text{Cos}[\omega t + k\,X(\varphi)]$$
$$= 2\,\text{Sin}\left[\frac{X(\varphi)-X(\theta_1)}{2}\right]\text{Sin}\left[\omega t+\frac{(2k-1)}{2}X(\varphi)+\frac{X(\theta_1)}{2}\right] \qquad [3\text{-}5]$$

Each newly formed output waveform has a common phase term given by $\frac{X(\theta_1)}{2}$ and a second phase term depending on k given by $(\frac{2k-1}{2})X(\varphi)$. Thus, the interpretation of an effective receiving phase center located at the center of the line adjoining the two elements.

The power response pattern of the newly formed element pair is then given by

$$b(\theta_1,\varphi) = \int_{-\infty}^{+\infty}\left[S_{k+1}(t) - S_k(t)\right]^2 dt$$
$$= 4\,\text{Sin}^2\left[\frac{X(\varphi)-X(\theta_1)}{2}\right]\int_{-\infty}^{+\infty}\text{Sin}^2\left[\omega t+\frac{(2k-1)}{2}X(\varphi)+\frac{X(\theta_1)}{2}\right] dt \qquad [3\text{-}6]$$
$$= 2\,\text{Sin}^2\left[\frac{X(\varphi)-X(\theta_1)}{2}\right]$$

Several typical response patterns are plotted in Figures 3-2 a, b, and c for various values of $\frac{d}{\lambda}$ and several values of θ_1. The response of each element pair is obviously null when $X(\varphi) = X(\theta_1)$ [i.e., $\varphi = \theta_1 \pm \pi$] regardless of the value of $\frac{d}{\lambda}$. The null in this newly formed

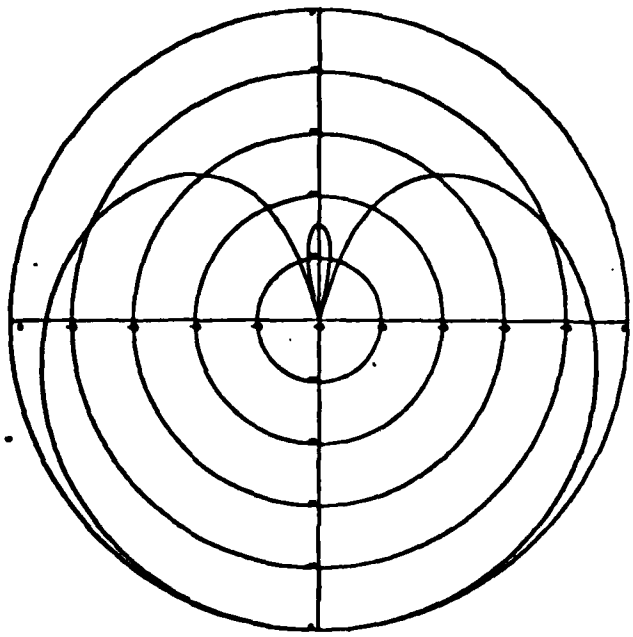

d=.1λ

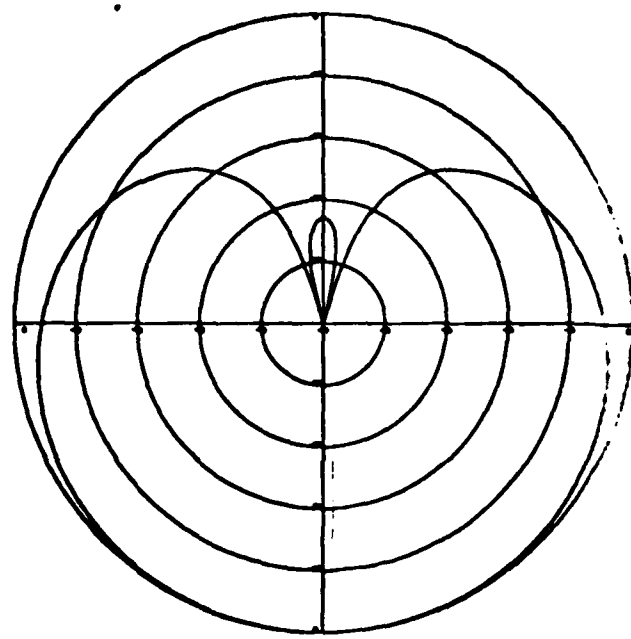

d=.2 λ

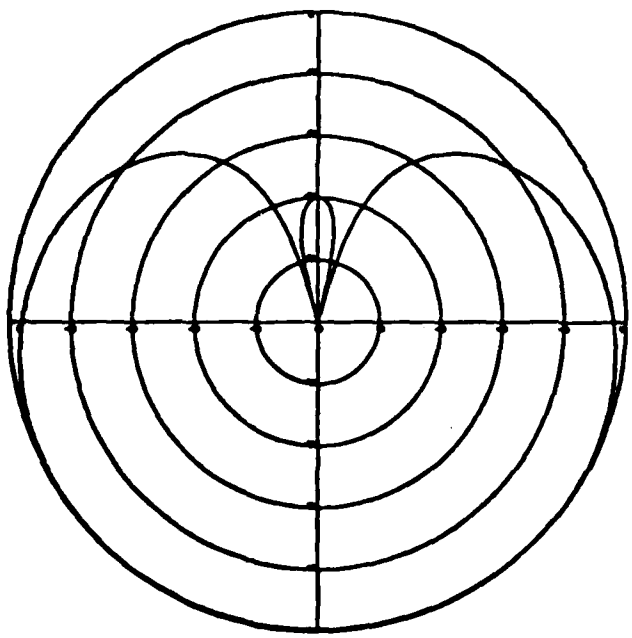

d=.3λ

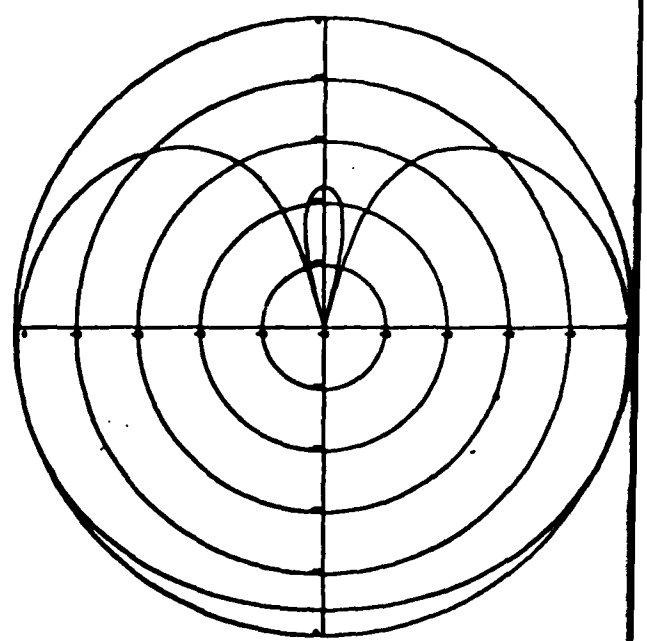

d=.4 λ

FIG. 3-2A ONE NULL DIRECTIONAL RECEIVING PATTERNS FOR EACH ELEMENT PAIR (θ_1-15°).

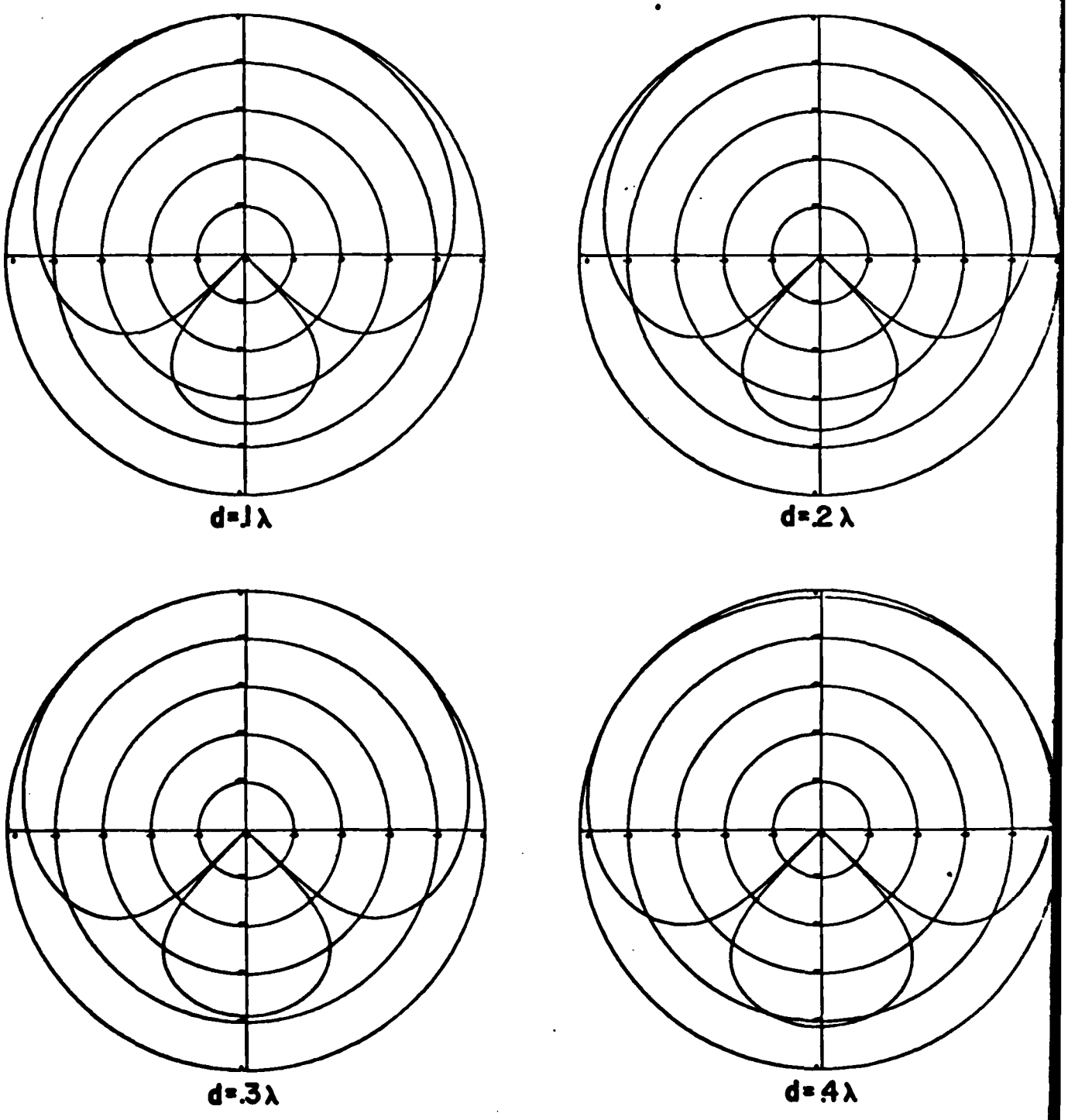

FIG. 3-2C ONE NULL DIRECTIONAL RECEIVING PATTERNS FOR EACH ELEMENT PAIR (θ_1-135°).

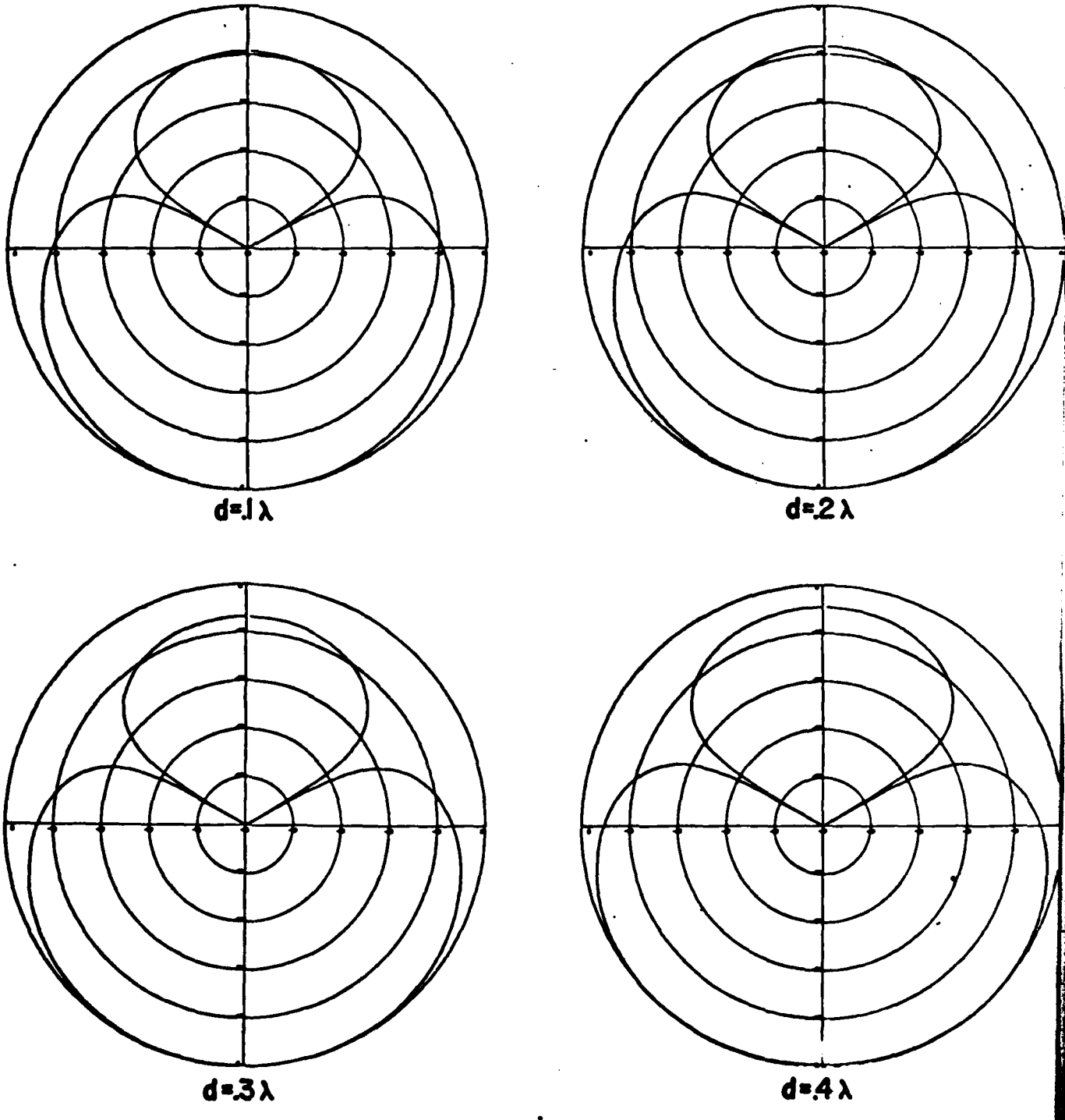

FIG. 3-28 ONE NULL DIRECTIONAL RECEIVING PATTERNS FOR EACH ELEMENT RAIR (θ_1-60°).

receiving pattern for each of the N-1 element pairs is thus capable of eliminating interfering sources of any bandwidth which arrive from the angle θ_1. The mirror symetry of the null is due to the symetry of the two element line arrays used to derive the directional receiving elements. The null is actually conconical about the axis joining the two elements.

3.2 Formation of Directional Receiving Elements With Multiple Nulls

Directional receiving phase centers having multiple nulls may be derived by a simple extension of the system shown in Figure 3-1 to the system shown in Figure 3-3 for two nulls.

As Figure 3-3 illustrates, the outputs of the directional elements with one null may be delay compensated so that a second interfering source arriving from an angle $\varphi = \theta_2 \neq \theta_1$ is in phase at adjacent outputs that are alternately either delayed by τ_2 or not delayed by τ_2. These adjacent output pairs are subtracted to form an effective receiving phase center which contains two nulls at $\varphi = \theta_1$ and $\varphi = \theta_2$. The delay τ_2 is simply given by

$$\tau_2 = \frac{d}{c} \cos\theta_2 \qquad [3\text{-}7]$$

since for the line array geometry shown the effective receiving phase centers after the first null is steered are still separated by $X(\varphi)$.

From equation 3-5, the outputs of two adjacent directional receiving outputs which have a null in the direction $\varphi = \theta_1$ may be obtained;

$$S'_k(t) - S_{k+1}(t) = 2 \sin\left[\frac{X(\varphi)-X(\theta_1)}{2}\right] \sin\left[\omega t + \left(\frac{2k-1}{2}\right)X(\varphi) + \frac{X(\theta_1)}{2}\right]$$

and [3-8]

$$S'_{k+1}(t) - S_{k+2}(t) = 2 \sin\left[\frac{X(\varphi)-X(\theta_1)}{2}\right] \sin\left[\omega t + \left(\frac{2k+1}{2}\right)X(\varphi) + \frac{X(\theta_1)}{2}\right]$$

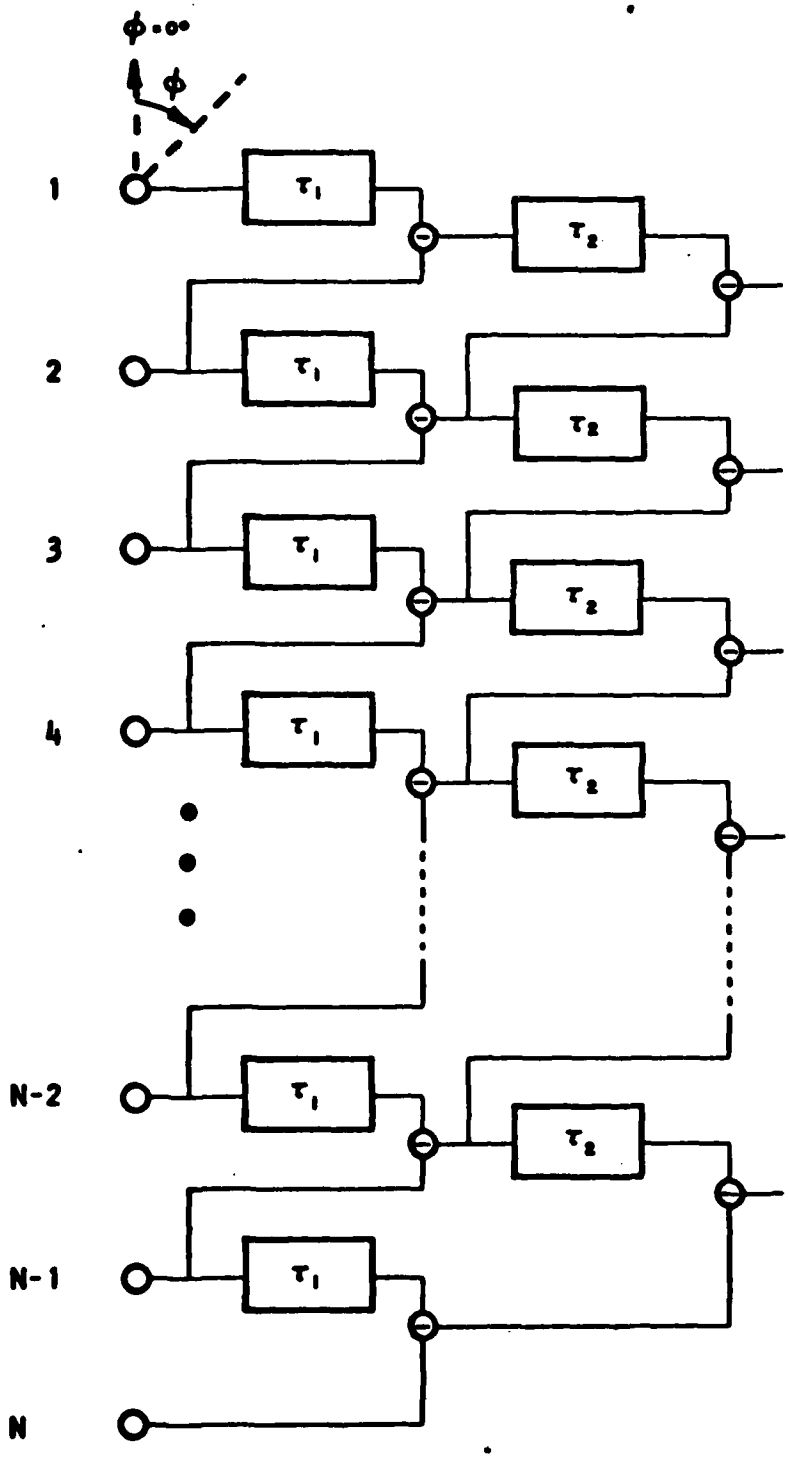

FIG. 3-3 SCHEMATIC REPRESENTATION OF A TWO NULL PROCESSOR.

TRACOR DWG A6-62-3039 2/22/69 SHORT

From Fig. 3-2 it can be seen that a second delay τ_2 is added to $S_k'(t) - S_{k+1}(t)$, and $S_{k+1}'(t) - S_{k+2}(t)$ is then subtracted from this delayed output. As in Eq. [3-4] and [3-5] the output of this second difference junction may be found thusly:

$$\left[S'_k(t) - S_{k+1}(t)\right]' - \left[S'_{k+1}(t) - S_{k+2}(t)\right]$$

$$= 2 \sin\left[\frac{X(\varphi)-X(\varphi_1)}{2}\right]\left\{\sin\left[\omega t+\left(\frac{2k-1}{2}\right)X(\varphi) + \frac{X(\theta_1)}{2} + X(\theta_2)\right]\right. \qquad [3\text{-}9]$$

$$\left. - \sin\left[\omega t + \left(\frac{2k+1}{2}\right) + \frac{X(\theta_1)}{2}\right]\right\}$$

$$= 2 \sin\left[\frac{X(\varphi)-X(\varphi_1)}{2}\right]\left\{2 \sin\left[\frac{X(\theta_2)-X(\varphi)}{2}\right] \sin\left[\omega t+kx(\varphi)+ \frac{X(\theta_1)}{2} + \frac{X(\theta_2)}{2}\right]\right\}$$

As before there is a common phase term for all two null outputs given by $\frac{X(\theta_1)+X(\theta_2)}{2}$ and a term depending on k which is given by $kx(\varphi)$. From Eq. [3-2] it is easy to see that the newly formed directional element output given by [3-9] has a phase center identical to the k+1 original omnidirectional element output. Each output after two nulls have been steered is separated from its neighboring output by the phase $X(\varphi)$. The power response pattern for the two null directional element output is obtained by squaring Eq. [3-9] and integrating over time as in Eq. [3-6].

$$b(\theta_1, \theta_2, \varphi) = 8 \sin^2\left[\frac{X(\varphi)-X(\theta_1)}{2}\right] \sin^2\left[\frac{X(\varphi)-X(\theta_2)}{2}\right] \qquad [3\text{-}10]$$

where the identity Sin(-X) = -Sin(X) has been used. Figures 3-4 a, b, and c present several typical response patterns for various values of d/λ and several combinations of values of θ_1 and θ_2.

The concepts presented in this section may be extended to provide directional receiving phase centers with any number of nulls less than N. In general if M nulls are steered there are N-M effective directional element outputs available for alignment and summing of the signal.

3.3 Beamformation from the N-M Interference Free Outputs

The preceeding subsections described the generation of N-M interference free outputs. The following paragraphs describe various ways that these outputs may be utilized to form beams with major response axes pointing in the desired directions. Only one scheme for the utilization of the N-M outputs is treated extensively, time shifting and summing. Other techniques have not as yet been thoroughly examined, but they are simple conceptual applications of beamforming techniques which have been implemented in the past.

3.3.1 Time-Shift and Sum Beamforming with the N-M Outputs

The N-1 interference free outputs provided by the processing scheme indicated by figure 3-1 may be time shifted such that the signal components at the N-1 outputs are in phase and then summed to form a beam. For the line array configuration treated in Section 3.1 and 3.2 the delays required to align the signal components at the N-1 outputs are quite simply related to the array element locations. From Eq. [3-5] it was seen that the effective spatial receiving phase centers of the N-1 outputs were located at the midpoint of the line adjoining the element pairs. Therefore, a signal arriving from a direction φ_o and received by an element pair produces an output which is different in phase from the adjacent output by $X(\varphi_o) = \frac{2\pi d}{c} \text{Cos } \varphi_o$. For the N-1 outputs,

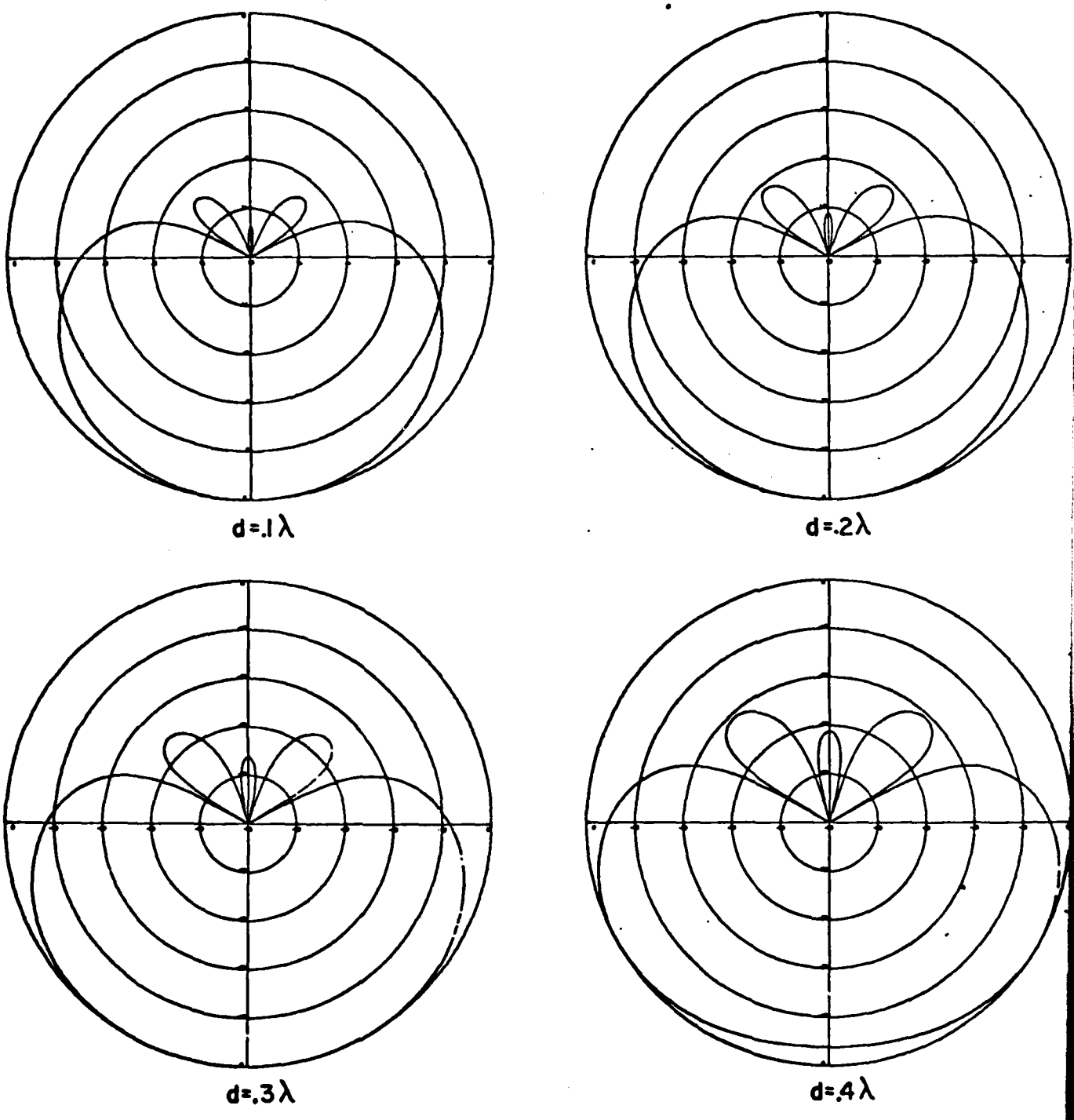

FIG. 3-4A TWO NULL DIRECTIONAL RECEIVING PATTERN FOR ELEMENT TRIPLETS (θ_1 ~~60°~~ 15° θ_2 ~~135°~~ 60°).

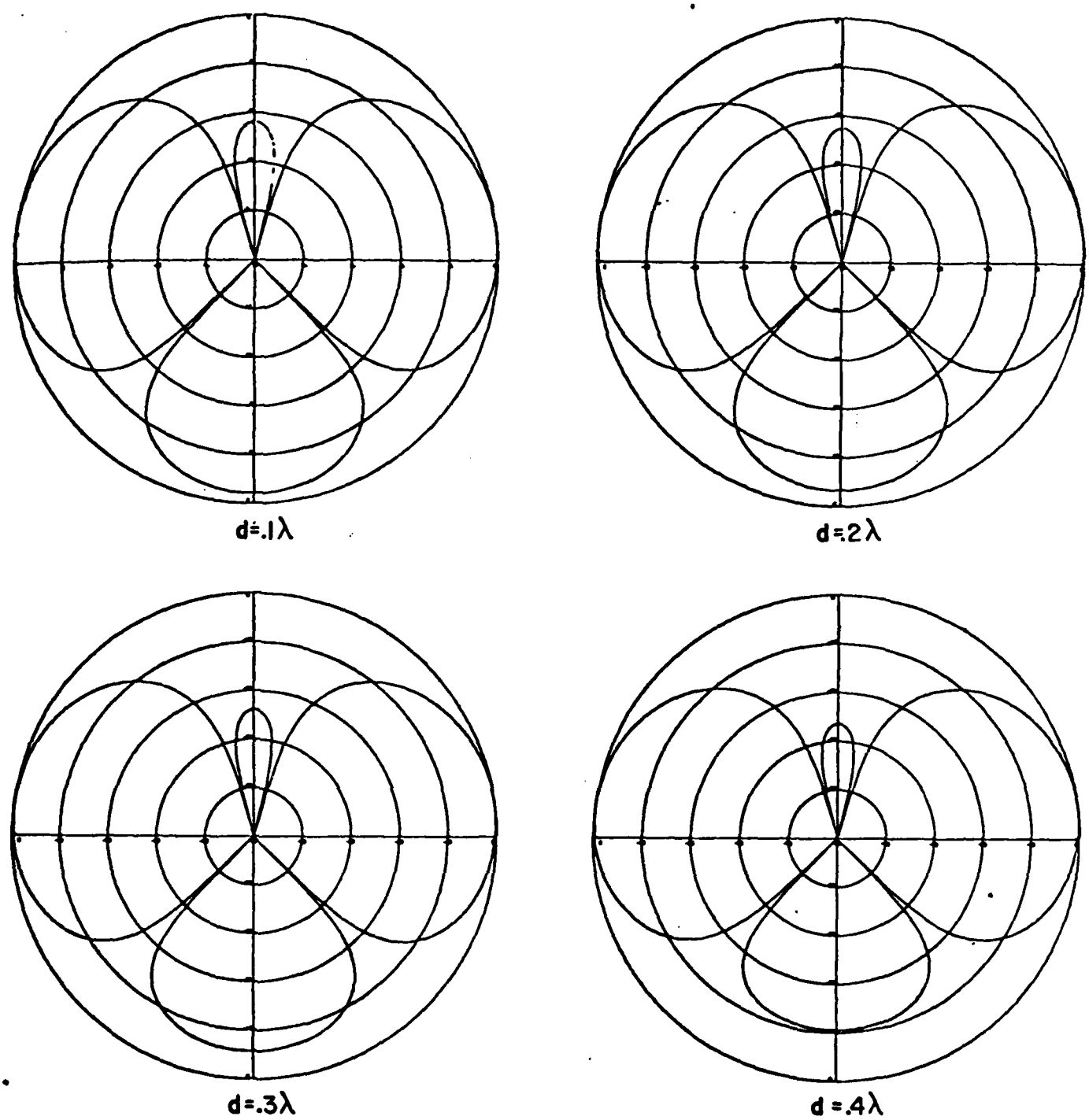

FIG. 3-4B TWO NULL DIRECTIONAL RECEIVING PATTERN FOR ELEMENT TRIPLETS (θ_1 ~~60°~~ 15° θ_2 135°).

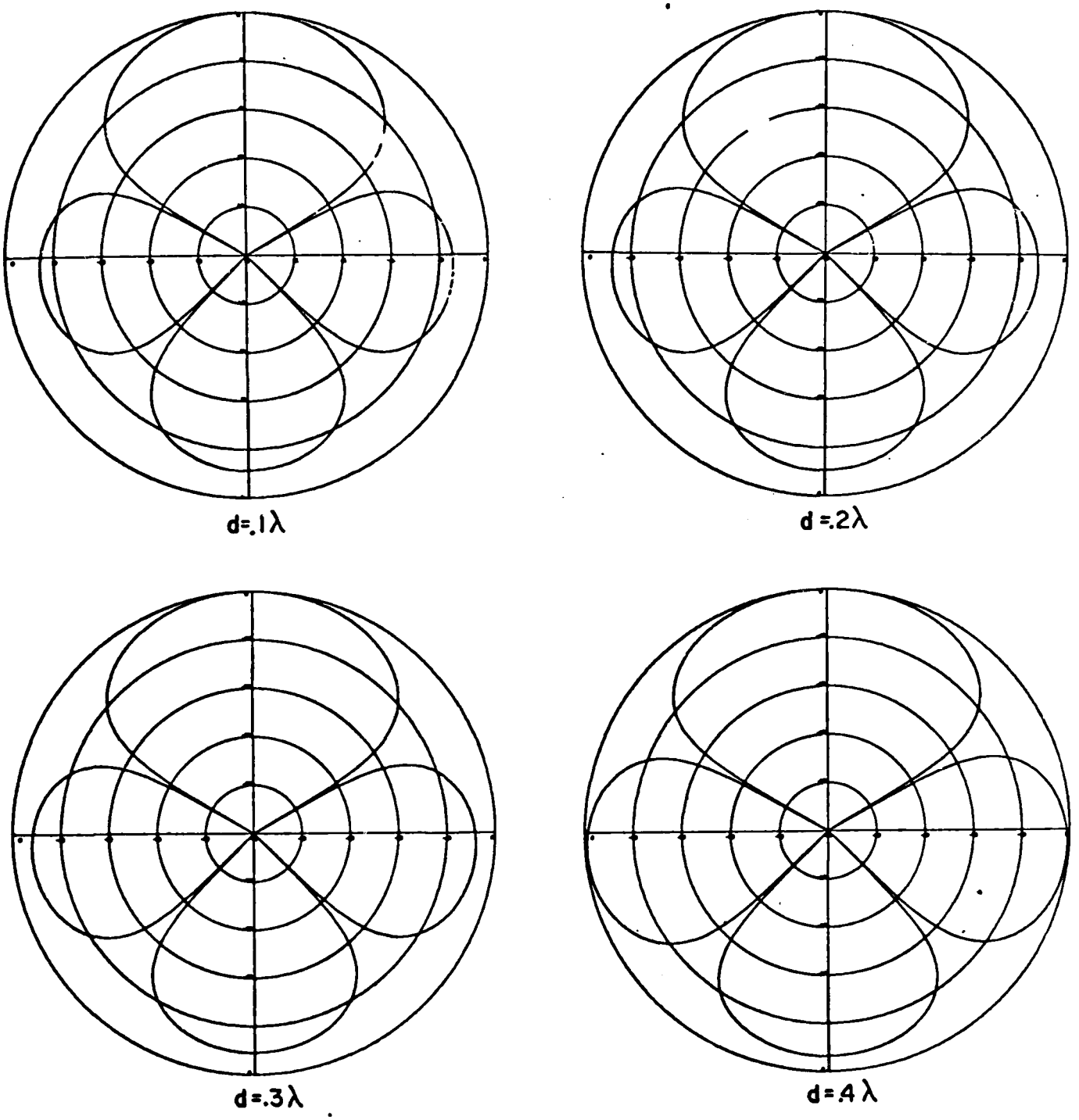

FIG. 3-4C TWO NULL DIRECTIONAL RECEIVING PATTERN FOR ELEMENT TRIPLETS (θ_1=60° θ_2=135°)

the relative delays are specified from some arbitrary zero phase reference. Let this reference be the first element in the array. The relative delays for the L = N-1 outputs are then given by

$$T_j = \frac{d(L-j)}{c} \text{Cos } \varphi_o \qquad j = 1, 2, 3 \ldots L \qquad [3\text{-}11]$$

Thus, the interference removal and beamforming processing is schematically represented by Figure 3-6 by extending Figure 3-1.

The L = N-2 outputs derived in Section 3.2 may be similarly utilized to form beams pointing in the desired directions by appropriately delaying the L outputs by the T_j's given by Eq. [3-11] where j = 1, 2, 3, . . . L where L = N-2. Section 4 contains several examples of such a utilization of these N-M outputs.

3.3.2 Other Beamforming Techniques Applied to the N-M Outputs

Instead of simply time shifting and summing the N-M outputs provided by the null steering it is in general possible to weight the nulled outputs in a prescribed manner to control the beam patterns. Some form of Tchebyscheff or Taylor shading could be applied prior to time-shifting and summing to control the side lobe levels or the major lobe width. Another approach which is used extensively today in many applications is clipped element beamforming. The N-M outputs may be clipped, sampled, time delayed and then summed to provide time normalized digital beam outputs. The present feeling is that the nulling technique would be implemented as multi-bit digital shift registers (or some other form of digital storage) and after null steering has taken place it would be beneficial to retain only the sign bit (clip) in order to simplify the beamforming and to guarantee a time-normalized system thereafter. In this manner the benefits of clipping can be obtained without suffering the detrimental

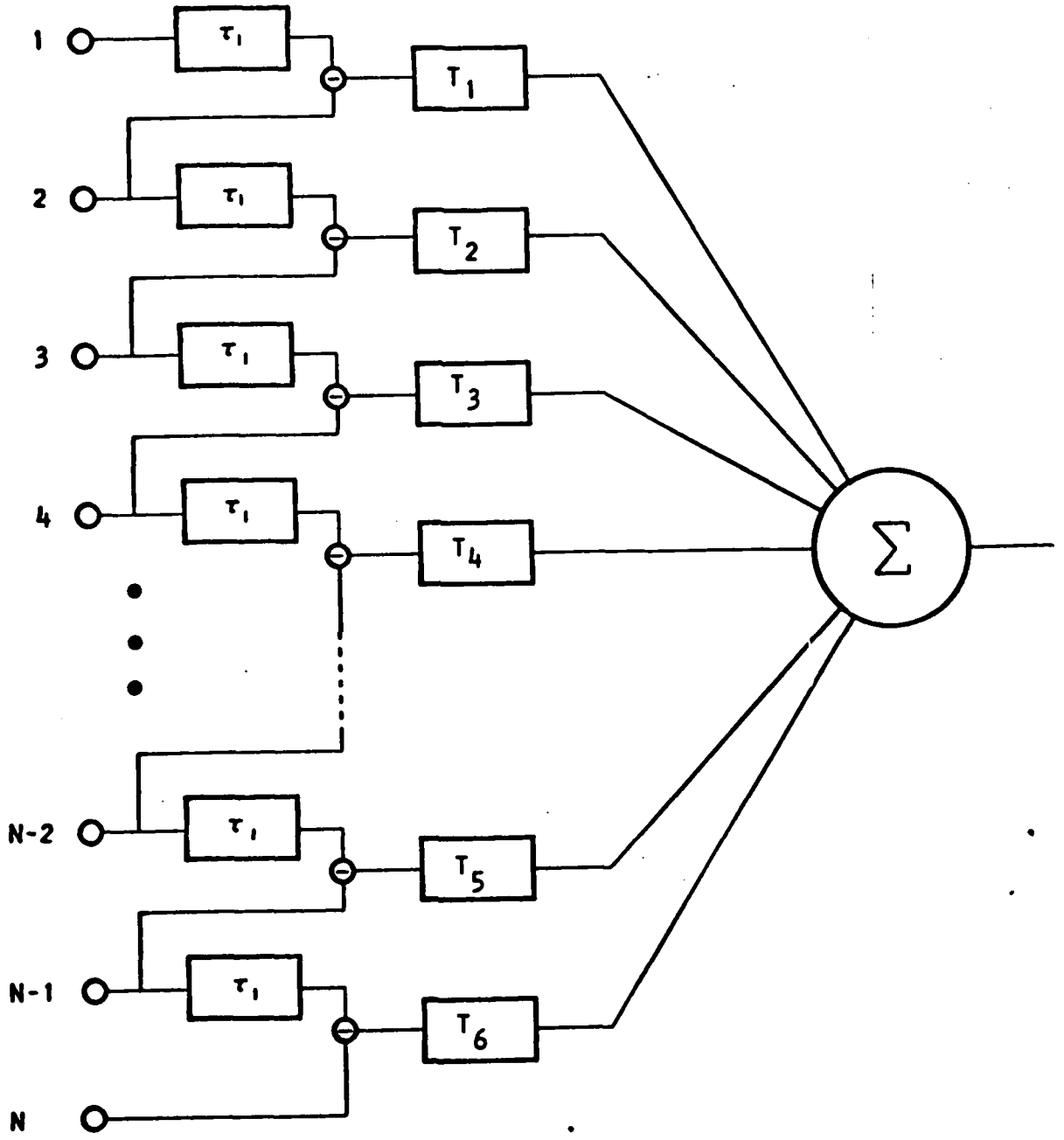

FIG. 3-6 SCHEMATIC REPRESENTATION FOR BEAMFORMING WITH N-1 OUTPUTS.

properties of clipping in the presence of high level plane wave interference which may drive the clipped system into a non-linear or even a saturated condition.

4. EXAMPLES OF TIME SHIFT AND SUM BEAMFORMING AFTER STEERING ONE AND TWO NULLS WITH A SIX ELEMENT LINE ARRAY

A simple computer model has been developed to allow examination of the beam patterns and array gain of (1) a classical time shift and sum beamforming and (2) a null steering and then time shift and sum beamforming of the N-1 or N-2 outputs in the presence of plane wave interfering noise sources. The processing represented in Fig. 3-6 and a simple time shift and sum beamforming of the N omnidirectional elements may both be represented as a system of linear filters; and the computer model is implemented from the viewpoint of a multi channel filtering system. The model is described below in Subsection 4.1 and the results of the model are described in Subsection 4.2.

4.1 Description of Model

The noise field is described in the frequency domain as an isotropic background plus one or two plane wave interfering noise sources. The cross spectral density matrix due to the total noise field, $\overline{C_{k\ell}(\omega)}$, is described by the cross spectral density matrix at the output of the N = 6 omnidirectional point receiving elements. Each element $C_{k\ell}(\omega)$ of the noise matrix is given by the sum of the cross spectral density due to the isotropic noise plus the cross spectral density due to each of the one or two interfering plane wave noise sources. Thus

$$C_{k\ell}(\omega) = C^{u}_{k\ell}(\omega) + \sum_{j=1}^{m} C^{I_j}_{k\ell}(\omega) \qquad [4\text{-}1]$$

where $C^{u}_{k\ell}(\omega)$ is the cross spectral density between elements k and ℓ due to the isotropic noise and $C^{I_j}_{k\ell}(\omega)$ is the cross spectral density between elements k and ℓ due to the plane wave interfering source I_j; and m is the number of interfering noise sources (1 or 2).

Now,

$$C^{u}_{k\ell}(\omega) = P^{u}(\omega) \frac{\text{Sin} \frac{(\ell-k)d\omega}{c}}{\frac{(\ell-k)d\omega}{c}} , \qquad [4\text{-}2]$$

where $P^{u}(\omega)$ is the isotropic noise spectrum in the water, and

$$\sum_{j=1}^{m} C^{I_j}_{k\ell}(\omega) = \sum_{j=1}^{m} I_j(\omega) \exp\left[\frac{i\omega(\ell-k)d \text{ Cos } \theta_j}{c}\right] \qquad [4\text{-}3]$$

where $I_j(\omega)$ is the spectrum of the j^{th} interfering noise source in the water.

The total noise power out when the filters, $h_k(\omega)$, k = 1,2, . . . N, given by the system represented in Fig. 3-6 or a simple time shift and sum beamformer, are applied is given by

$$\int \overline{[\text{row } h^{*}_{k}(\omega)]} \; \overline{C_{k\ell}(\omega)} \; \overline{[\text{col } h_{\ell}(\omega)]} \, d\omega = \int C_{o}(\omega) d\omega \qquad [4\text{-}4]$$

where * denote the complex conjugate.

The signal is described by a single plane wave arrival at the array. The cross spectral density matrix due to the signal, $\overline{S_{k\ell}(\omega)}$, at N omnidirectional outputs is given by the elements

$$S_{k\ell}(\omega) = S(\omega) \exp\left[\frac{i\omega(\ell-k) \; d\text{Cos}\varphi_s}{c}\right] , \qquad [4\text{-}5]$$

where φ_s is the signal arrival direction and S(ω) is the signal spectrum in the water.

The total signal power out of the beamformer is given by

$$\int \overline{[\text{row } h^{*}_{k}(\omega)]} \quad \overline{S_{k\ell}(\omega)} \quad \overline{[\text{col } h_{\ell}(\omega)]} d\omega = \int S_{o}(\omega) \quad . \qquad [4\text{-}6]$$

The beam patterns were obtained by letting φ_s vary from 0^o to 359^o in 1^o steps and computing [4-6] at each step. The array gain is determined by computing equation [4-6] divided by [4-4] and dividing this by the signal-to-noise ratio in the water.

4.2 Simulation Results

The model was run for a set of single frequencies over a two octave band. The frequency was varied by varying the ratio of element spacings to wavelength, d/λ , from 0.1 to 0.4 in steps of 0.1. Thus the integrals in [4-4] and [4-6] did not have to be performed. The beampatterns for a simple time shift and sum beamforming are presented in Figure 4-1. The beampatterns for steering one null and then time shift and summing are presented in figure 4-2a, b, and c for null steering directions of 15^o, 60^o, and 135^o respectively. The beam patterns for steering two nulls and then time shift and summing are presented in Figures 4-3a, b, and c for combinations of two null steering directions of 15^o and 60^o; 15^o and 135^o; and 60^o and 135^o respectively.

Figures 4-4a, b, and c are graphs of the array gain defined by

$$\text{Array Gain} = \frac{\text{signal-to-total noise power ratio at the beamformer output}}{\text{signal-to-total noise power ratio in the water}} ,$$

versus interference-to-isotropic background noise ratio $(I/N)w$ in the water for both a classical time shift and sum beamformer and a null steering then time shift and sum beamformer. A set of four curves for the four values of d/λ is presented for each beamforming technique. The signal and beam boresight are located at $180^o(\varphi_s)$ and the interference arrival directions (φ_I) for figures 4-4a, b, and c are 15^o, 60^o, and 135^o respectively. The signal-to-isotropic background noise ratio is -20dB. When $(I/N)w$ is small (i.e. the interference-to-signal ratio is greater than the difference between the side lobe level and the major

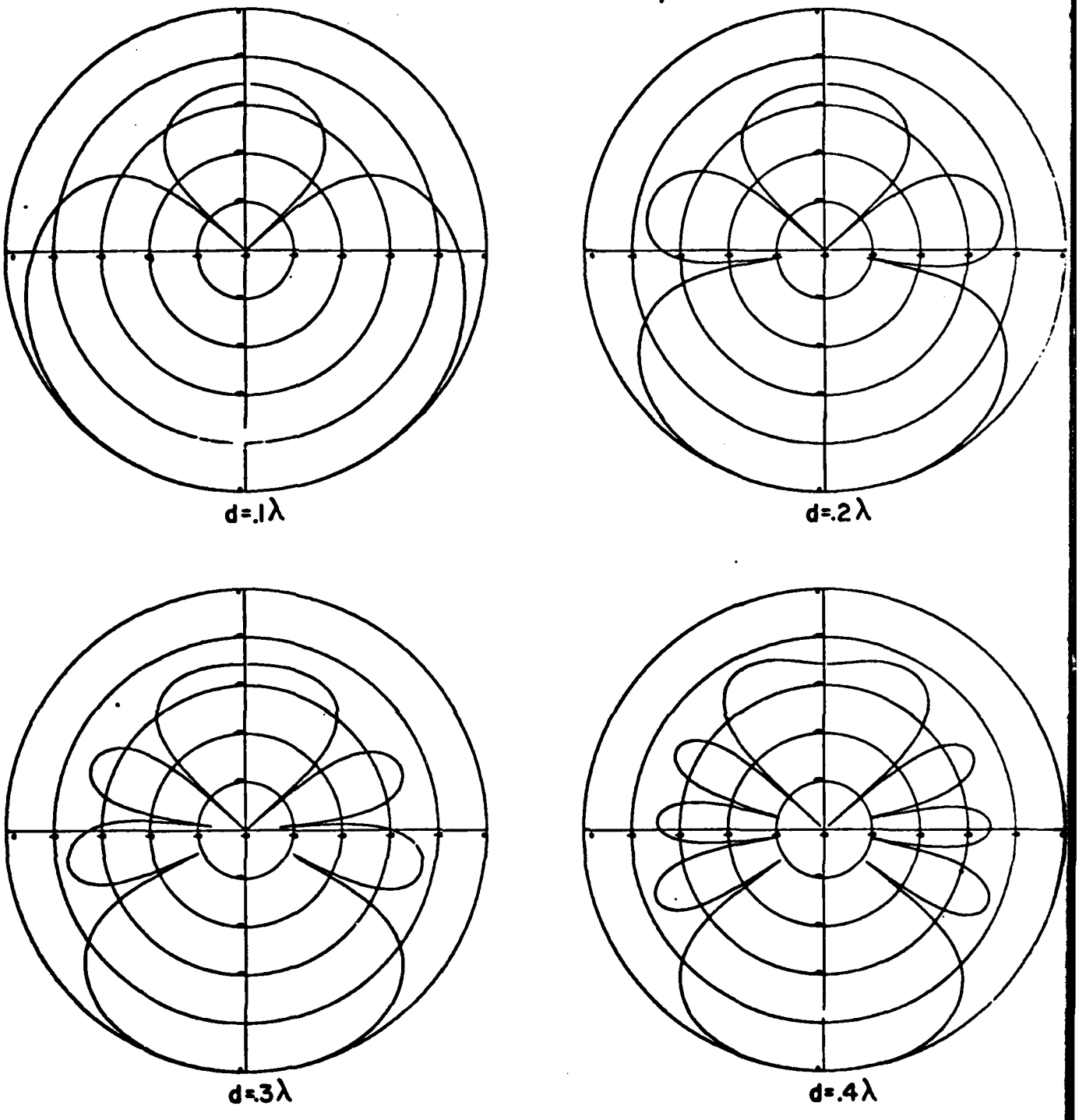

FIG. 4-1 BEAM PATTERNS FOR 6 ELEMENTS
TIME-SHIFT AND SUM BEAMFORMING.

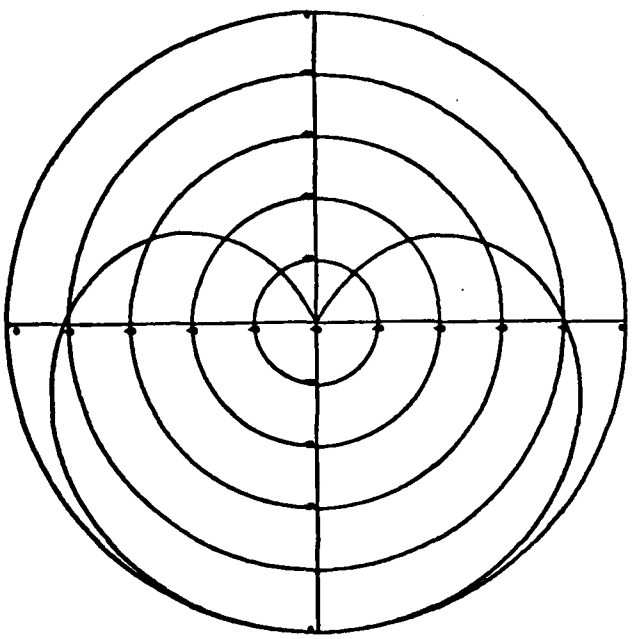

d=.1λ

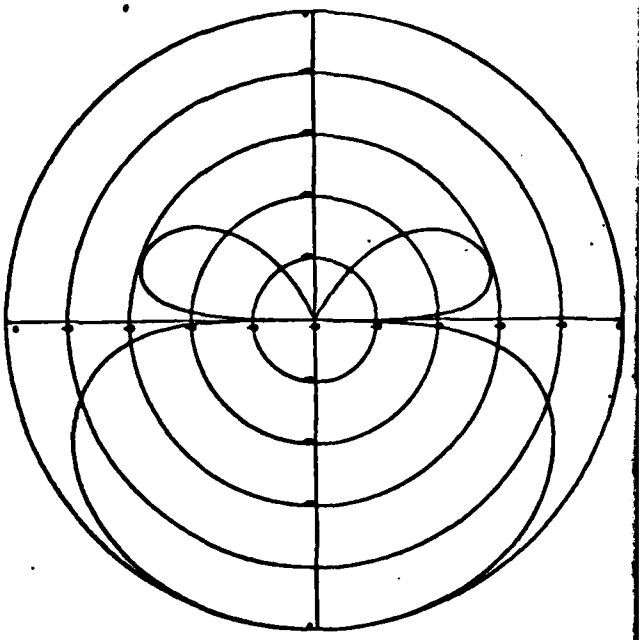

d=.2λ

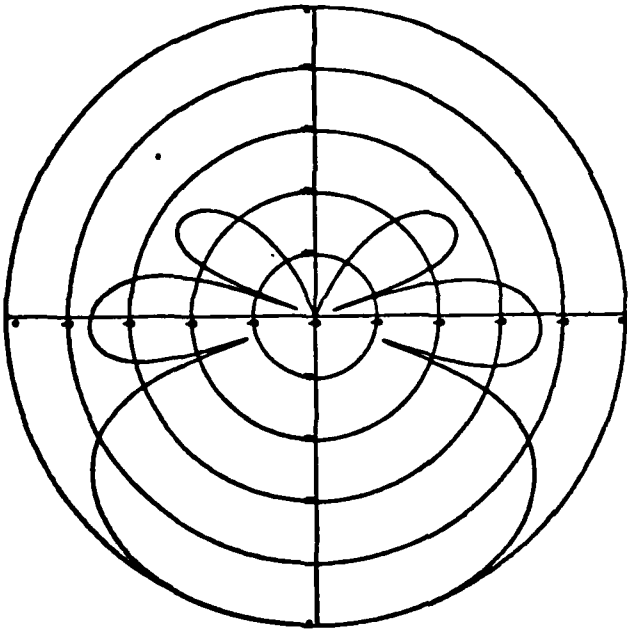

d=.3λ

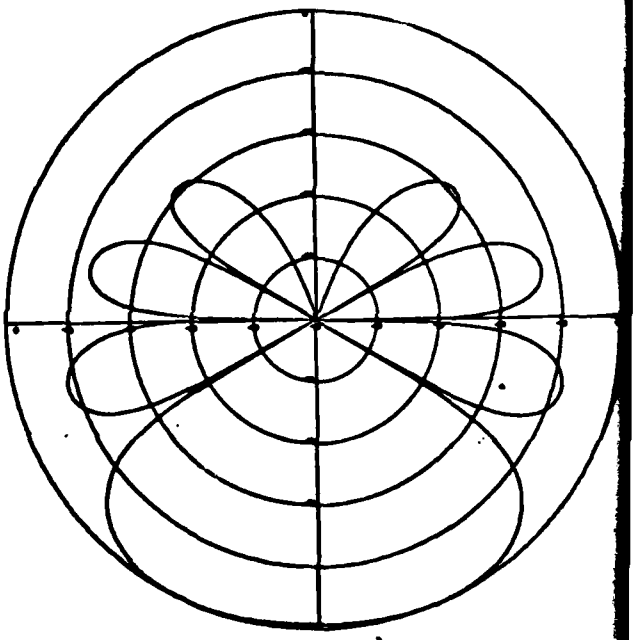

d=.4λ

FIG. 4-2A BEAM PATTERNS FOR ONE-NULL, TIME-SHIFT AND SUM BEAMFORMING (θ_1=15°).

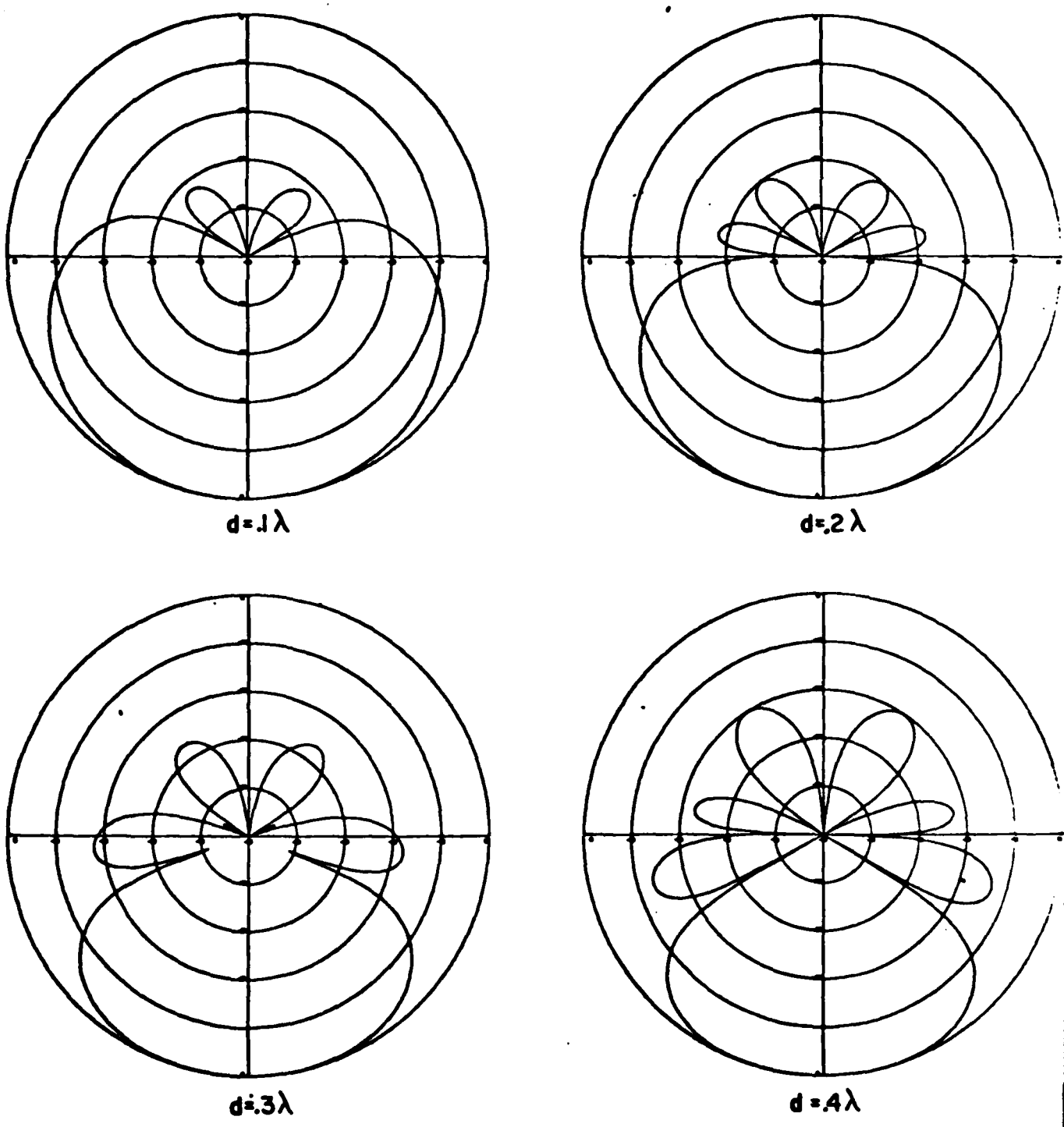

FIG. 4-28 BEAM PATTERNS FOR ONE-NULL, TIME-SHIFT AND SUM BEAMFORMING (θ_1=60°).

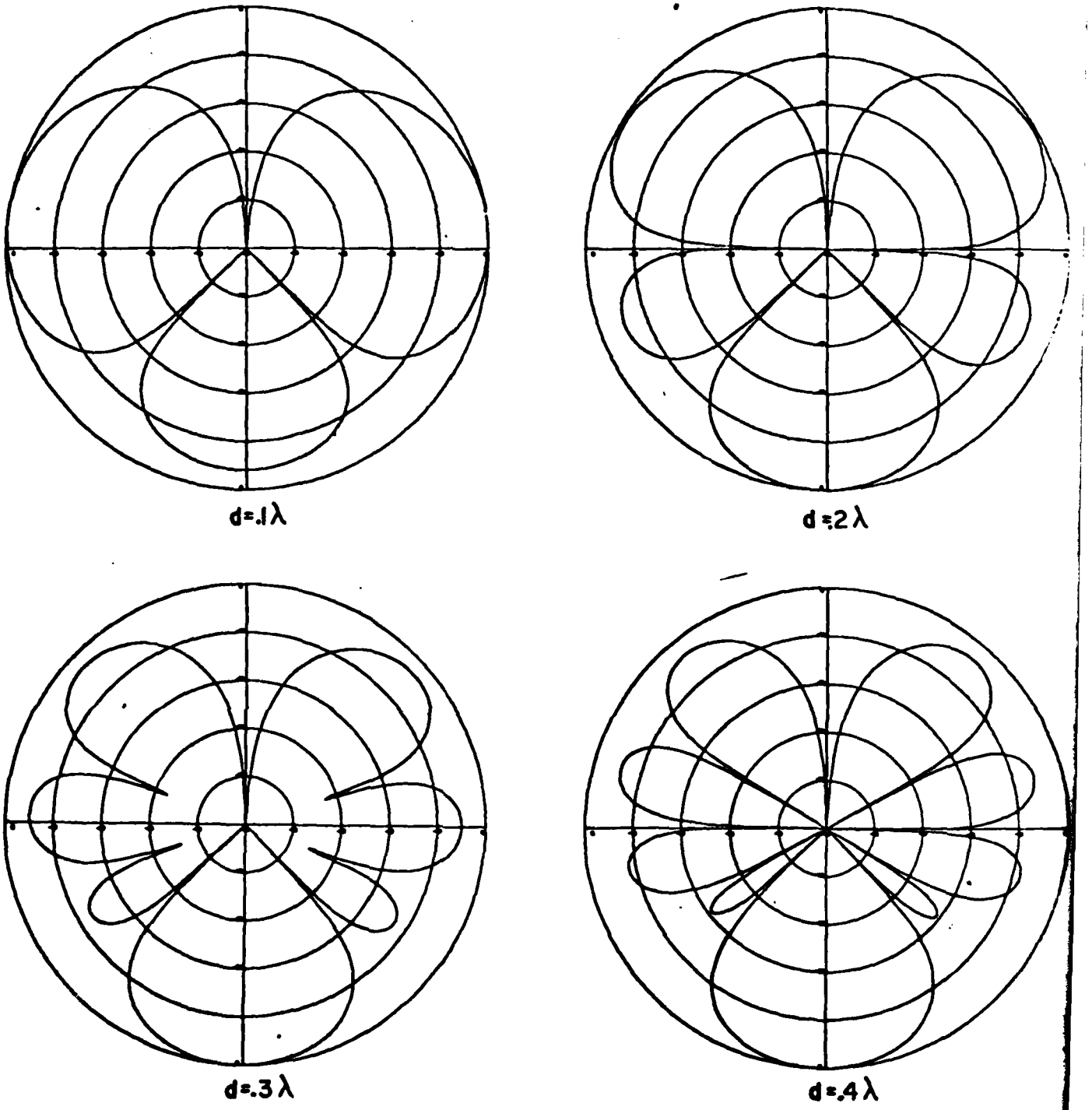

FIG. 4-2C BEAM PATTERNS FOR ONE-NULL, TIME-SHIFT AND SUM BEAMFORMING (θ_1=135°).

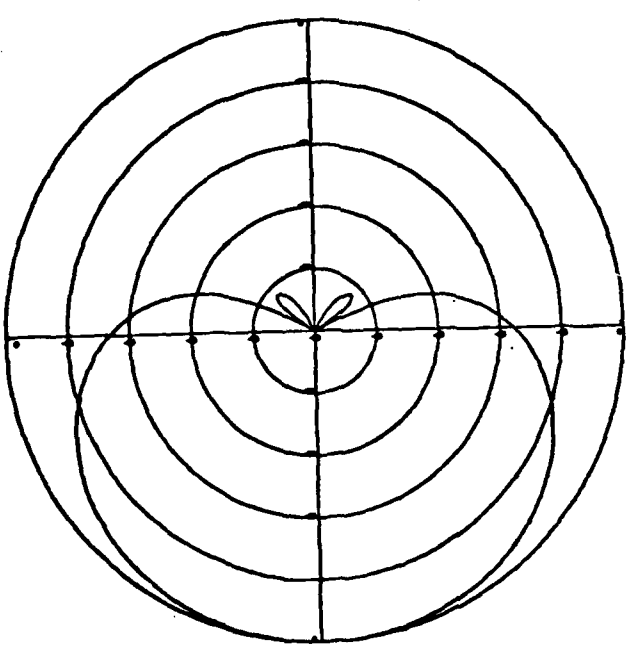

d=.1λ

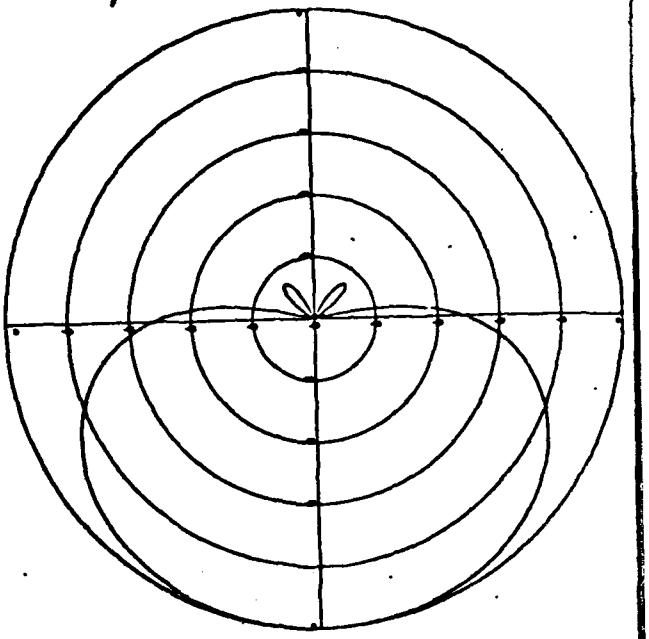

d=.2λ

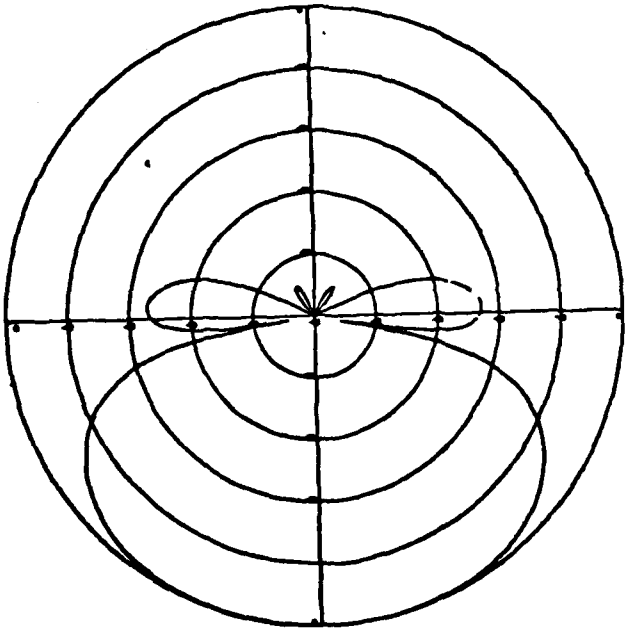

d=.3λ

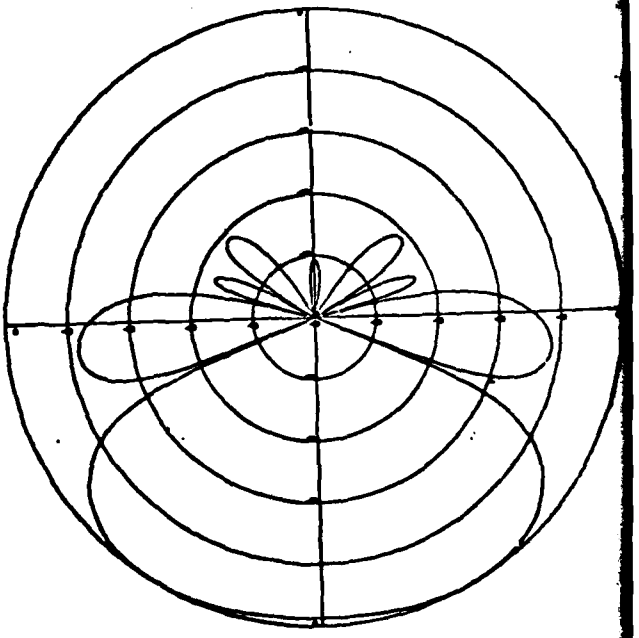

d=.4λ

FIG. 4-3A BEAM PATTERNS FOR TWO-NULLS, TIME-SHIFT AND SUM BEAMFORMING (θ_1=15°, θ_2=60°).

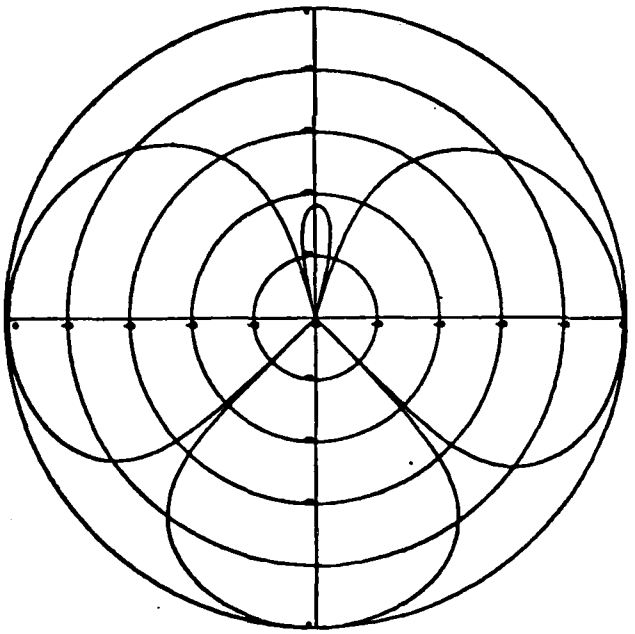

d=.1 λ

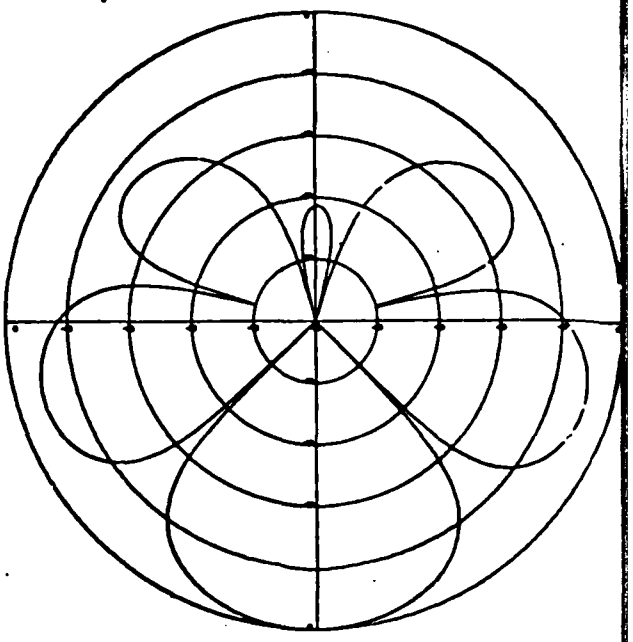

d=.2 λ

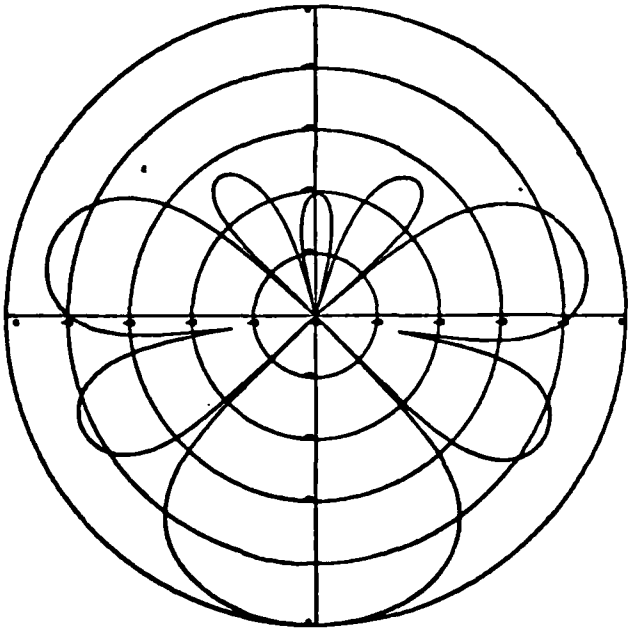

d=.3 λ

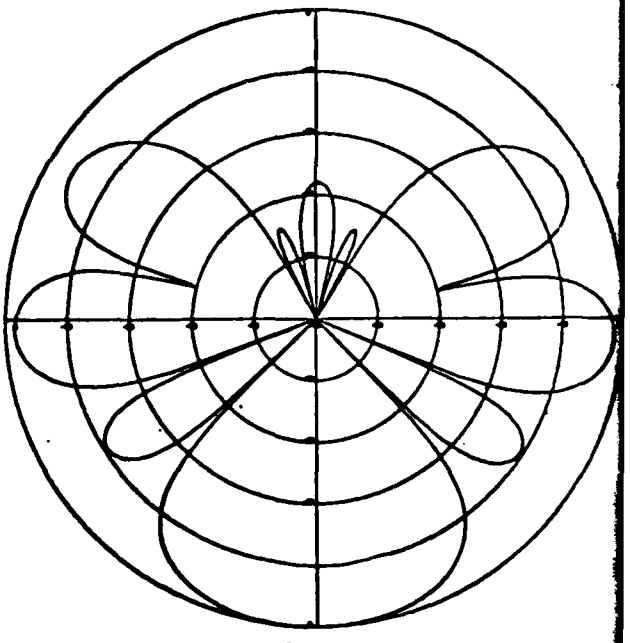

d=.4 λ

FIG. 4-38 BEAM PATTERNS FOR TWO-NULLS, TIME-SHIFT AND SUM BEAMFORMING (θ_1=15°, θ_2=135°).

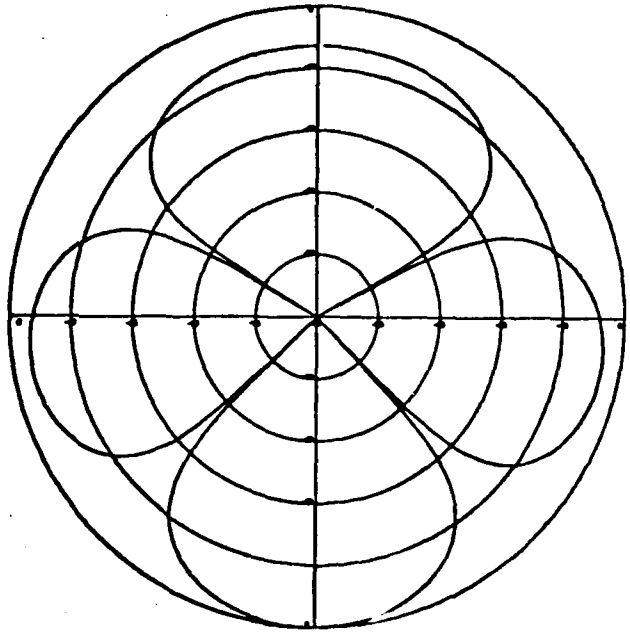

d=.1λ

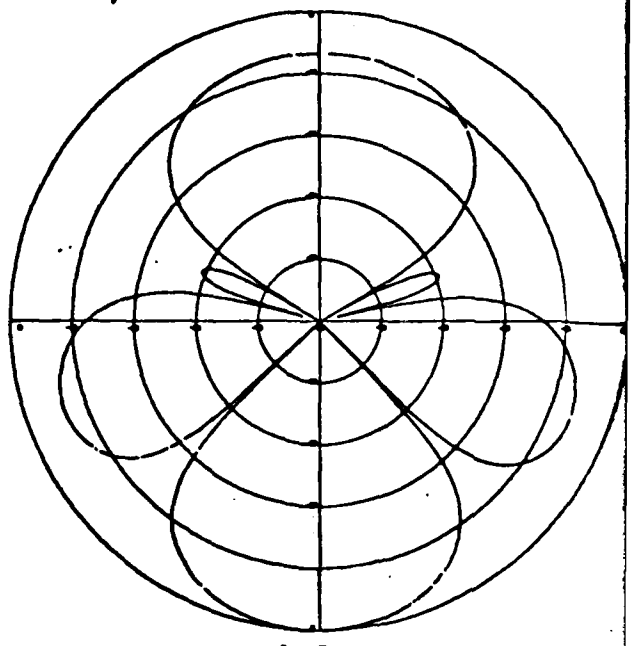

d=.2 λ

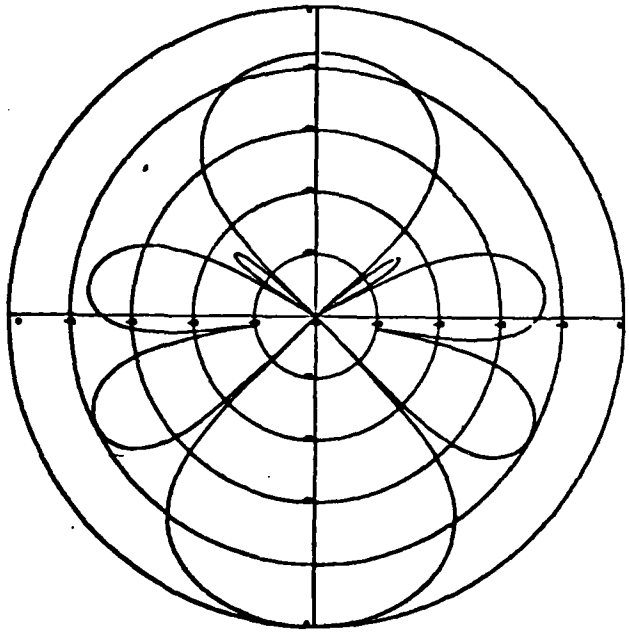

d=.3λ

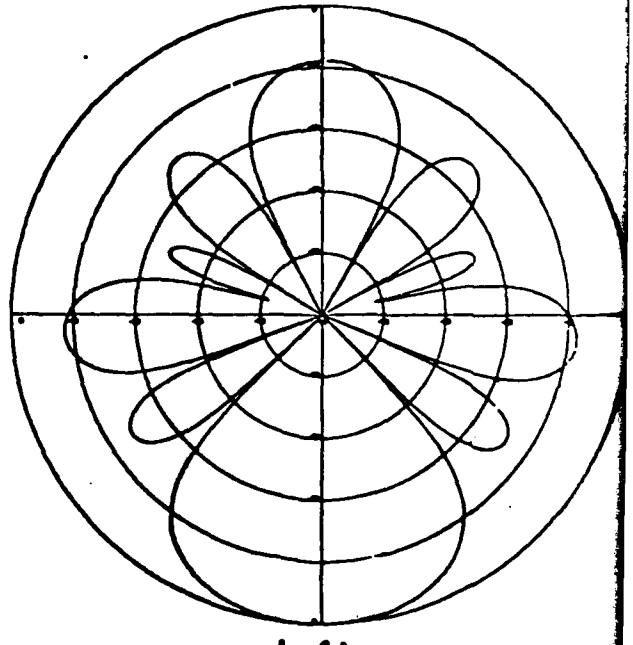

d=.4λ

FIG. 4-3C BEAM PATTERNS FOR TWO-NULLS, TIME-SHIFT AND SUM BEAMFORMING (θ_1-60°, θ_2-135°).

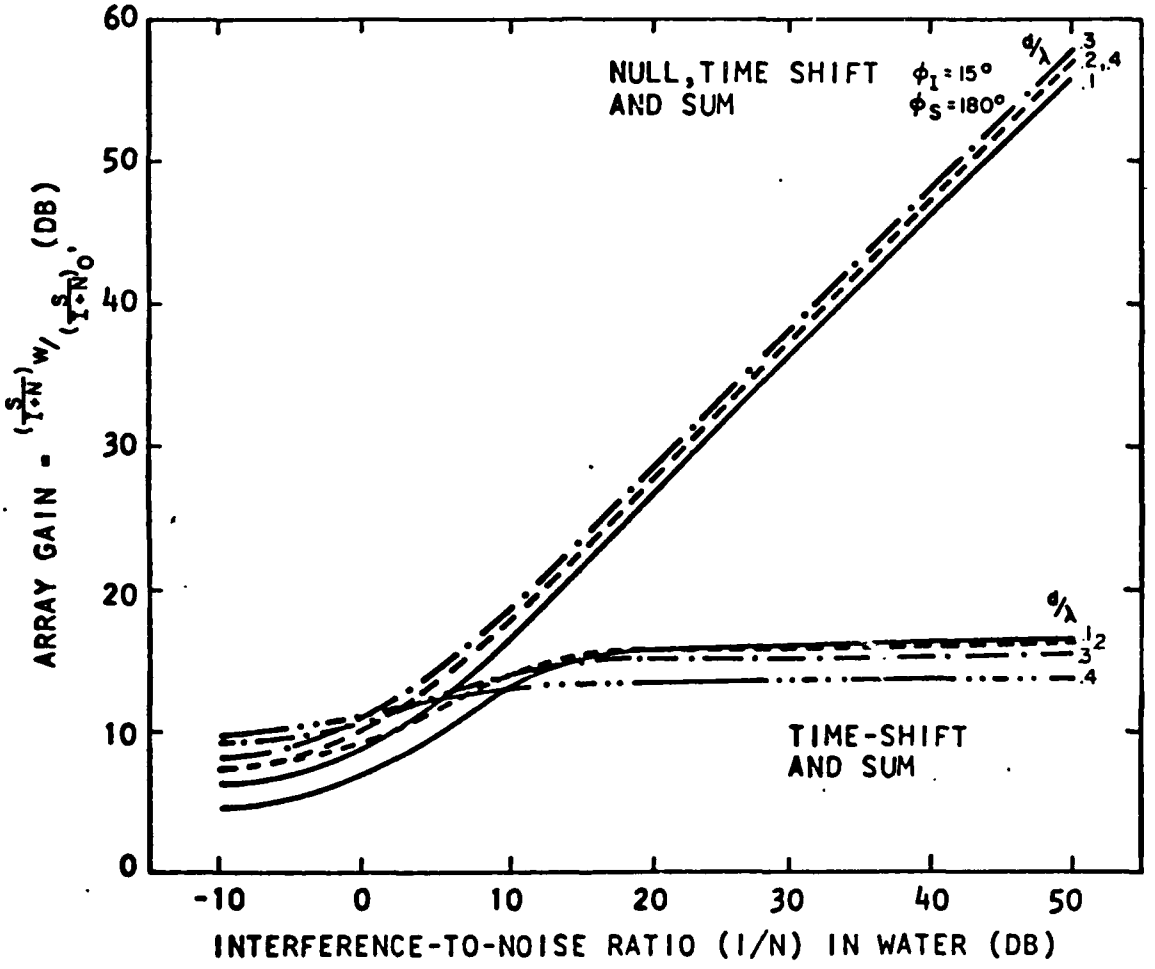

FIG.4-4A COMPARISON OF ARRAY GAIN VS. INTERFERENCE-TO-ISOTROPIC BACKGROUND NOISE RATIO IN THE WATER FOR A CLASSICAL TIME-SHIFT AND SUM BEAMFORMER AND A NULL STEERING PROCESSOR PRIOR TO TIME-SHIFT AND SUM BEAMFORMING.

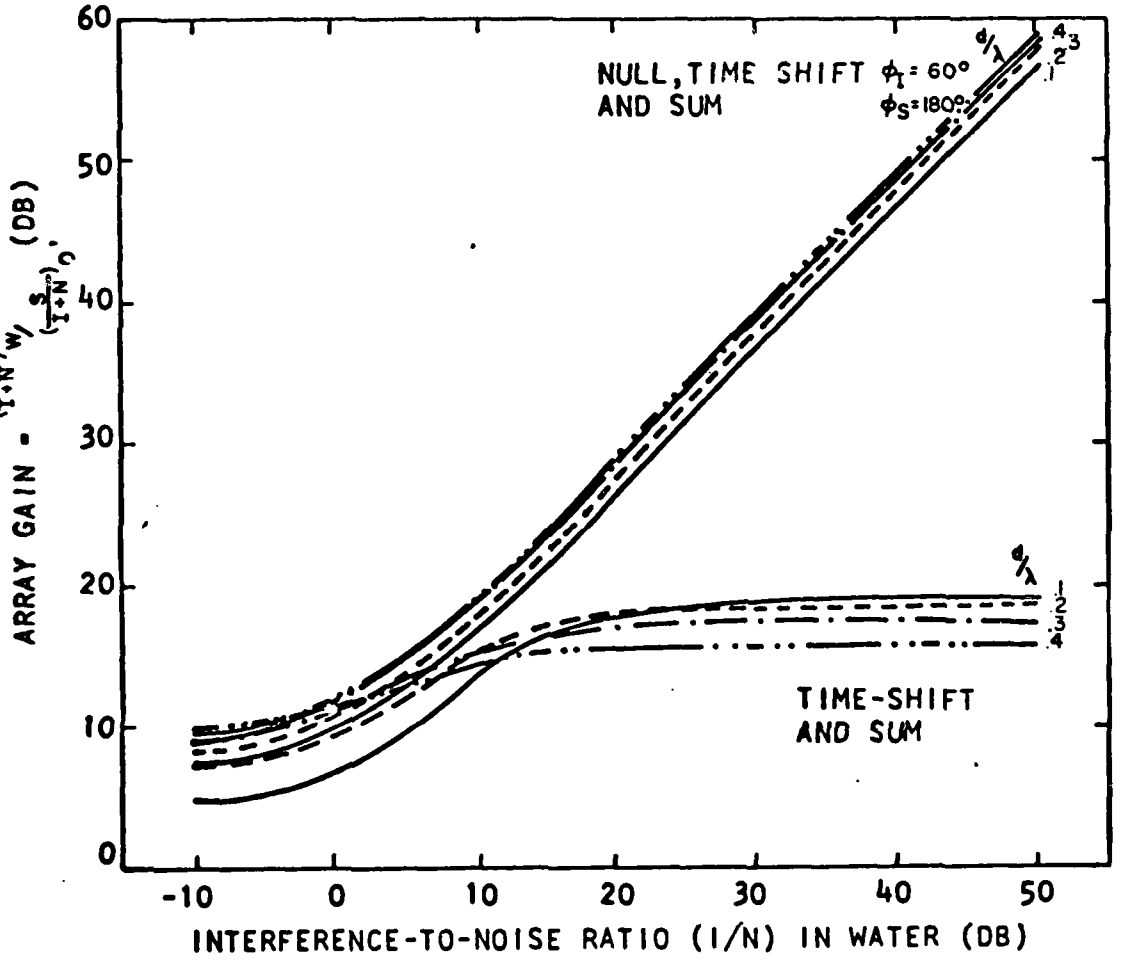

FIG.4-4B COMPARISON OF ARRAY GAIN VS. INTERFERENCE-TO-ISOTROPIC BACKGROUND NOISE RATIO IN THE WATER FOR A CLASSICAL TIME-SHIFT AND SUM BEAMFORMER AND A NULL STEERING PROCESSOR PRIOR TO TIME-SHIFT AND SUM BEAMFORMING.

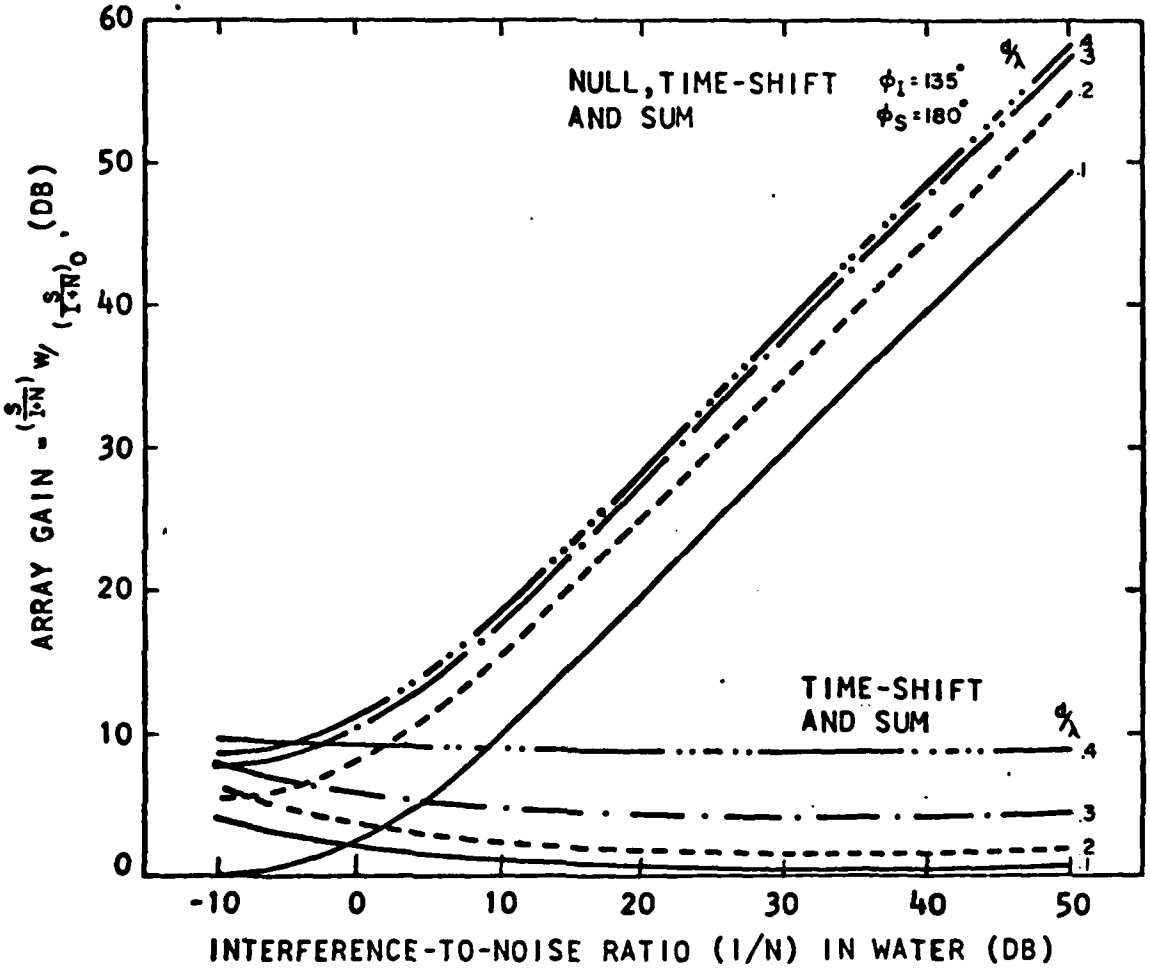

FIG.4-4C COMPARISON OF ARRAY GAIN VS. INTERFERENCE-TO-ISOTROPIC BACKGROUND NOISE RATIO IN THE WATER FOR A CLASSICAL TIME-SHIFT AND SUM BEAMFORMER AND A NULL STEERING PROCESSOR PRIOR TO TIME-SHIFT AND SUM BEAMFORMING.

response axis level) there is little difference in the array gain between the two beamforming techniques. For some combinations of null steering angles and values of d/λ the array gain at very low $(I/N)w$ ratios is larger for the classical time shift and sum beamformer. For other combinations of these parameters the null steering prior to time shift and sum beamforming gives higher array gain at low $(I/N)w$ ratios.

Whenever $(I/N)w$ becomes large compared to (S/N) the noise is increased at the output of the time shift and sum beamformer by the amount that the interference is increased in the water. Thus, the array gain for the classical time shift and sum technique limits at high interference levels. On the other hand the null steering prior to time shift and sum beamforming provides interference rejection. In other words the beam outputs for the null steering technique prior to beamforming do not contain power due to the interference. This is reflected in the array gain curve approaching a slope of unity since the null steering technique provides complete interference rejection (increased processing against the total noise) regardless of how much the interference level increases.

Figures 4-5 a, b, and c are graphs of the array gain versus interference-to-isotropic background noise ratio for the case of two interfering noise sources located at 15° and 60°; 15° and 135°; and 60° and 135° respectively. The comparison is for a classical time shift and sum beamformer and a two null steering process followed by a time shift and sum of the N-2=4 outputs. The two horizontal scales define the ratio of interference-to-isotropic background ratio for each of the two noise sources (I/N) and for the sum of $\left(\frac{I_1+I_2}{N}\right)$ of the two independent noise sources. The remaining parameters are as defined for Figures 4-4 a, b, and c. The only difference between the Figures 4-4 and 4-5 is that the interference is somewhat more degrading to the simple time shift and sum beamformer and thus, there is

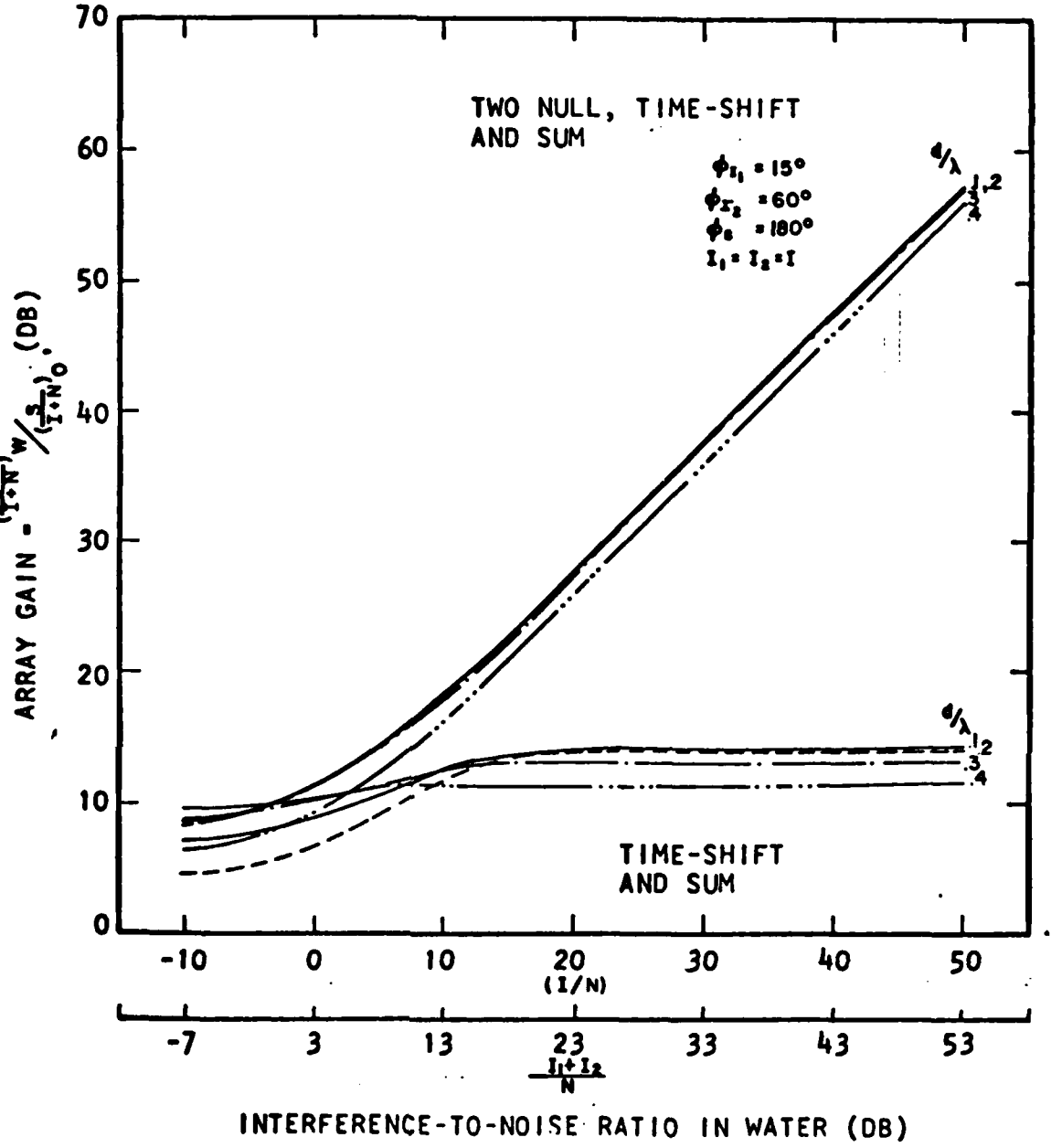

FIG.4-5A COMPARISON OF ARRAY GAIN VS. INTERFERENCE-TO-ISOTROPIC BACKGROUND NOISE RATIO IN THE WATER FOR A CLASSICAL TIME-SHIFT AND SUM BEAMFORMER AND A TWO NULL-STEERING PROCESSOR PRIOR TO TIME-SHIFT AND SUM BEAMFORMING.

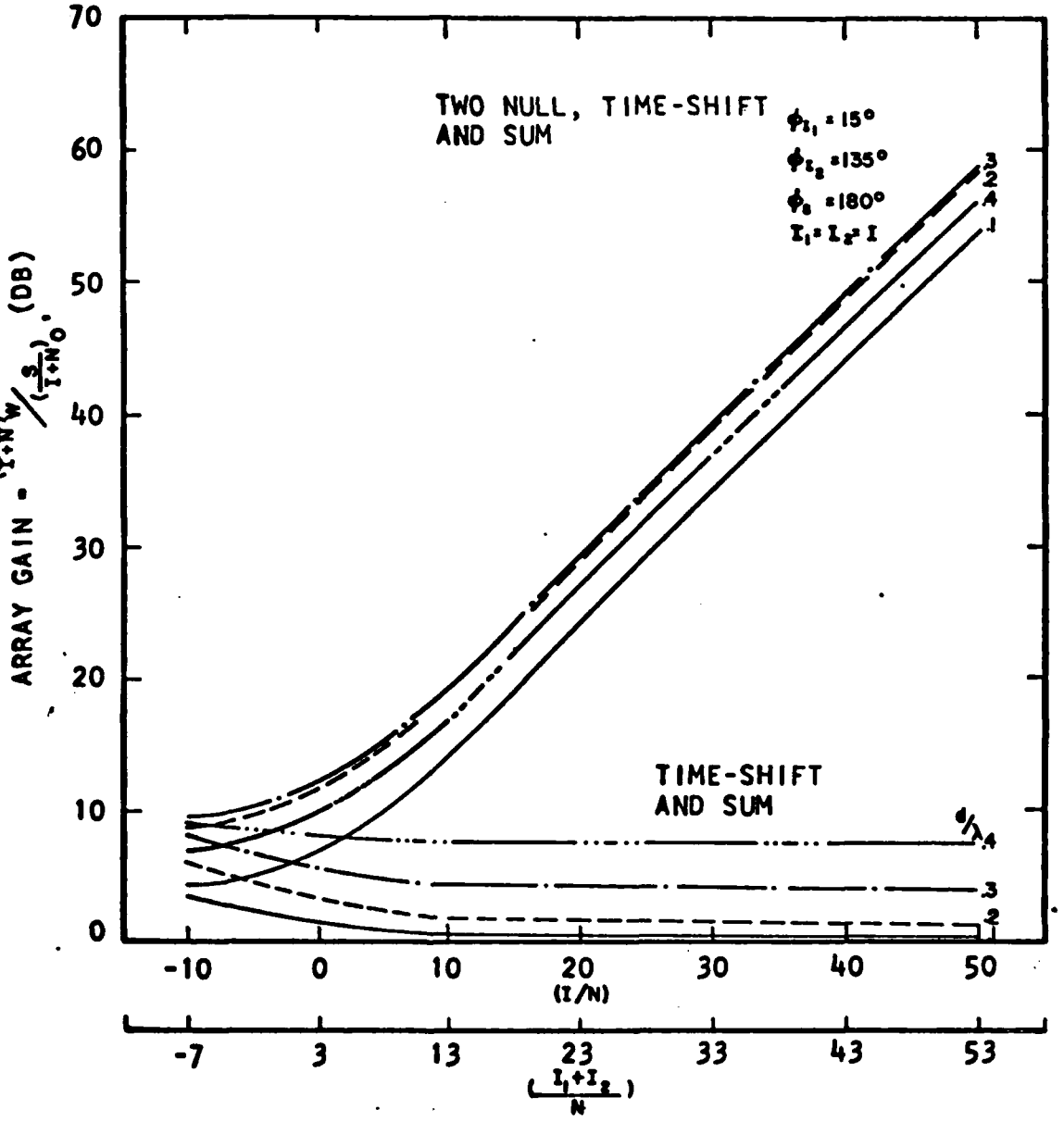

FIG.4-5B COMPARISON OF ARRAY GAIN VS. INTERFERENCE-TO-ISOTROPIC BACKGROUND NOISE RATIO IN THE WATER FOR A CLASSICAL TIME-SHIFT AND SUM BEAMFORMER AND A TWO NULL-STEERING PROCESSOR PRIOR TO TIME-SHIFT AND SUM BEAMFORMING.

TRACOR DWG A6-62-3092 2/25/69 SHORT

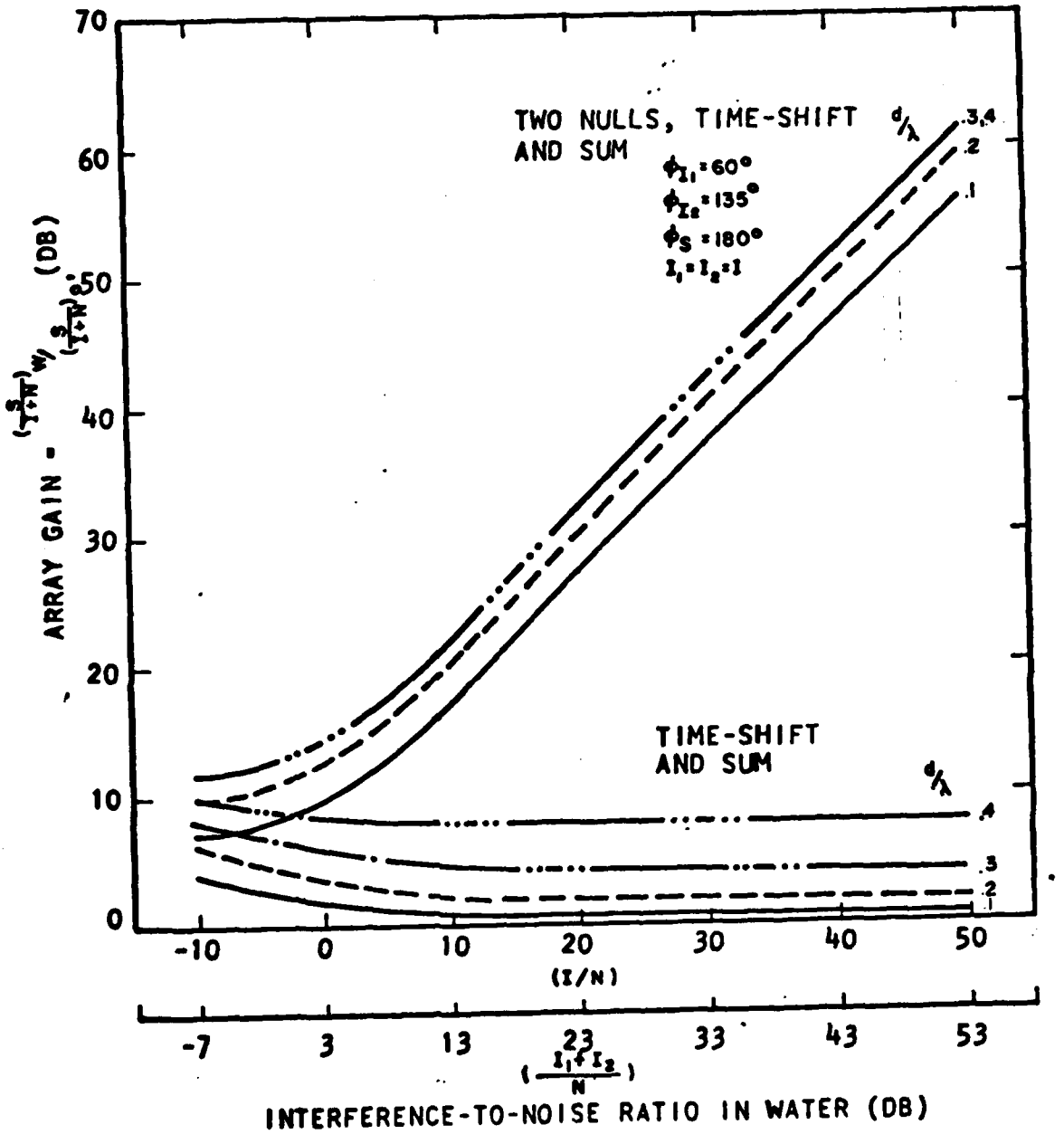

FIG.4-5C COMPARISON OF ARRAY GAIN VS. INTERFERENCE-TO-ISOTROPIC BACKGROUND NOISE RATIO IN THE WATER FOR A CLASSICAL TIME-SHIFT AND SUM BEAMFORMER AND A TWO NULL-STEERING PROCESSOR PRIOR TO TIME-SHIFT AND SUM BEAMFORMING.

TRACOR DWG A6-62-3095
2/19/69 SHORT

more advantage to steering nulls prior to the time shift and sum section of the beamformer.

REFERENCES

1. Morton Kanefsky, SUBIC Report, "Processing of Data From Sonar Systems," Volume IV, Supplement 1, December 27, 1967, General Dynamics Corporation Electric Boat Division for Office of Naval Research, (UNCLASSIFIED).

2. H. Mermoz, "Adaptive Filtering and Optimal Utilization of an Antenna," Bureau of Ships Translation No. 903, 4 October 1965, (UNCLASSIFIED).

3. H. Mermoz, "Elimination of Interfering Noisemakers by Optimum Antenna Processing," Given at Advanced NATO Conferences at Enschede, Holland, August 1968, (UNCLASSIFIED).